A PHYLOGENOMIC FRAMEWORK, EVOLUTIONARY TIMELINE, AND GENOMIC RESOURCES FOR COMPARATIVE STUDIES OF DECAPOD CRUSTACEANS

Joanna M. Wolfe, Jesse W. Breinholt, Keith A. Crandall, Alan R. Lemmon, Emily Moriarty Lemmon, Laura E. Timm, Mark E. Siddall, and Heather D. Bracken-Grissom

Proceedings of the Royal Society B, **doi:10.1098/rspb.2019.0079**

Extended Data:

1. Extended Methods:

(a) Whole genome sequencing and QC

To assist with probe design, whole genome sequencing (WGS) was conducted for nine exemplar decapod species (**Table S2**): *Panulirus argus* (Achelata: Palinuridae), *Coenobita clypeatus* (Anomura: Coenobitidae), *Emerita talpoida* (Anomura: Hippidae), *Procambarus clarkii* (Astacidea: Cambaridae), *Menippe nodifrons* (Brachyura: Menippidae), *Ocypode quadrata* (Brachyura: Ocypodidae), *Periclimenes rathbunae* (Caridea: Palaemonidae), *Penaeus duorarum* (Dendrobranchiata: Penaeidae), and *Stenopus hispidus* (Stenopodidea: Stenopodidae). These species were targeted as they span the phylogenetic breath of Decapoda, and could be freshly collected (or represented recently collected material). All material was selected from the Florida International Crustacean Collection (FICC) or newly collected in localities around southern Florida. All identifications were done by H. Bracken-Grissom using dichotomous keys for these groups.

DNA was extracted from gills, legs or abdominal muscle tissue using the Qiagen Blood and Tissue Extraction Kit following manufacturers' protocols. For these nine decapod lineages, low-coverage genome data were newly collected after DNA extracts were sonicated to a distribution of 200-500 bp and used to produce 8 bp single-indexed Illumina libraries following Lemmon et al. [1] and Prum et al. [2]. Libraries were pooled and sequenced on 18 PE-150 Illumina HiSeq2500 lanes with onboard clustering, producing 711 Gb of data (6x to 31x genomic coverage, **Table S2**). After sequencing, paired reads passing Illumina Casava High Chastity filter were merged following Rokyta et al. [3], i.e. if the paired reads overlapped at their 3' ends (updating quality scores for the overlapping positions, but leaving nonoverlapping bases unchanged). At this point, sequencing errors were corrected and library adapters were removed. These genomes were not assembled; the short reads were screened for probe design (discussed below).

(b) Transcriptome sequencing

Transcriptomes were sequenced from multiple developmental stages for each of four exemplar decapod species: *Homarus americanus* (Astacidea: Nephropidae), *Lysmata wurdemannii* (Caridea: Lysmatidae), *Mithraculus sculptus* (Brachyura: Mithracidae), and *Paralithodes camtschaticus* (Anomura: Lithodidae). For adult females, brain and/or muscle tissues were dissected. For embryos (mid-germband stage) and larvae (first zoea), several individuals were pooled into 1-3 replicates for each stage. Each sample was preserved in RNALater for transport to AMNH. Collecting and sample information are found in **Table S3**.

Total RNA was extracted separately from individual tissues. Prior to immersion in RNALater, whole animals were rinsed in 10% bleach followed by deionized water (to minimize microbial contaminants). Samples were separately macerated in Trizol using the Xpedition mechanical sample processor (Zymo Research), followed by RNA extraction with the Direct-zol kit (Zymo), including a poly-A binding step to isolate mRNA. The quality and quantity of mRNA was measured with the BioAnalyzer 2100 (Agilent) and Qubit 2.0 fluorometer

(Invitrogen). cDNA libraries were generated with TruSeq DNA preps (Illumina) at Weill Cornell Medical College (for *L. wurdemanni*) and the New York Genome Center (for the other three species). Transcriptomes were sequenced at the above respective labs, using Illumina HiSeq with 2x100 paired end reads, and 9-10 samples multiplexed per flow cell.

(c) Transcriptome QC and assembly

Raw Illumina reads were filtered for each sample using a Galaxy workflow based on the FASTQ toolkit, following [4]. Briefly, adapter sequences were removed, followed by FASTQ Groomer, removal of sequencing artifacts, and quality filtering. *De novo* transcriptome assembly of filtered reads, combining all sequenced samples of a species, used Trinity [5] with the default minimum k-mer threshold abundance (=1, so all k-mers were used in assembly). As in Alexandrou et al. [4], Trinity output was re-assembled using iAssembler [6]. The number of raw and filtered reads and assembly statistics are compiled in **Table S4**.

(d) Probe design

AHE targets conserved coding regions that are flanked by less conserved sequence regions, with the goal of optimizing phylogenetic informativeness at multiple levels of divergence [1]. Short probe sequences are hybridized to genomes of interest, and then those targeted regions are enriched prior to sequencing [1]. Capture efficiency depends strongly on the similarity between the probes and the genomes of interest, thus we created a new probe set targeting highly conserved regions in decapod genomes. Target AHE regions were identified at the FSU Center for Anchored Phylogenomics (www.anchoredphylogeny.com), using an approach similar to that successfully employed for other arthropod groups, including Diptera [7], Arachnida [8], Hemiptera [9], Coleoptera [10], Neuroptera [11], and Lepidoptera [12]. First, as few annotated genomes were available, genomic resources from 23 species representing a variety of Decapoda were obtained from published and new sources (see **Table 1** for an overview and **Table S1** for details), including the nine new genomic and four new transcriptome datasets described above. These were used as references for probe design.

To identify AHE target regions in Decapoda, genomic reads from two species (RefsA in **Table 1**) identified in preliminary tests to yield the highest sequence recovery, *Coenobita clypeatus* (Anomura: Coenobitidae) and *Procambarus clarkii* (Astacidea: Cambaridae) were mapped to reference sequences from *Tribolium castanaeum*. The *Tribolium* sequences were obtained from the Coleoptera AHE probe design alignments developed by Haddad et al. [10], who targeted 941 protein coding regions conserved across Insecta. The mapping process, which follows that described in detail by Hamilton et al. [8], identifies matching raw reads using a 17 bp of 20 bp spaced-k-mer threshold for preliminary matching, and 55% similarity score for final placement of a read. As in [8], each target region was required to be at least 150 bp in length, and containing no known exon boundaries. For each target region, reads matched by these criteria were aligned and then extended into flanking regions. For each target region, the obtained decapod sequences were aligned together with the corresponding *Tribolium* sequence using MAFFT v7.023 [13]. Geneious R9 (Biomatters Ltd.; [14]) was used to identify and select well-aligned regions that were utilized downstream. This process resulted in 823 preliminary AHE

target regions for decapods, based on sequences from the references *T. castanaeum*, *C. clypeatus* and *P. clarkii*.

To expand references across six selected decapod 'major lineages' (Achelata, Anomura, Astacidea, Brachyura, Caridea, and Dendrobranchiata), we scanned six assembled transcriptomes (RefsB in **Table 1**, including the four newly sequenced transcriptomes above, as well as *Litopenaeus vannamei* (Dendrobranchiata: Penaeidae) and *Cherax quadricarinatus* (Astacidea: Parastacidae [15])) for the 823 preliminary AHE target regions. Following Hamilton et al. [8], we identified for each preliminary AHE target the best-matching transcript (with 55% match minimum) in each of the six transcriptomes, to establish target regions. The resulting sequences were aligned using MAFFT [13] and inspected in Geneious. After selecting the well-aligned regions and removing 21 poorly aligned sequences, targets represented in fewer than four of the six selected major decapod lineages were removed from downstream analyses. Removal of overlapping loci (identified as having one or more shared 60-mer for any species) resulted in 352 final AHE targets, which contained both exonic and intronic regions.

Unlike previous studies of vertebrate and terrestrial arthropod clades [1,2,7-12], decapods diverged over 450 million years ago (e.g. **Figure 3**). Therefore, our initial investigations revealed that a single probe set covering all of this evolutionary history was not practical if we wanted to sequence a sufficient number of target regions per species. The remaining genomic resources were therefore utilized to build alignments representing the diversity within each of the six selected major lineages. Raw reads from 16 additional species (see **Table S1**) were mapped to major lineage-specific reference sequences (developed above) and used to extend the resulting sequences into flanking regions [8]. The best matching genomic region in the assembled *Neocardina denticulata* genome (Caridea: Atyidae; [16]) was also identified (4000 bp containing each region was utilized downstream). For each AHE target region x major lineage combination (n = 352 targets x 6 major lineages), an alignment containing all of the recovered sequences (together with the major lineage-specific reference sequence) was then generated using MAFFT and inspected in Geneious. As each alignment contained at least one sequence derived from a genome, we were able to identify and mask intronic regions. To improve capture efficiency, we also masked repetitive regions identified using k-mer counts in the *N. denticulata* genome. This was done by creating a database for each species using all 15-mers found in the trimmed probe region alignments, and all 15-mers that were 1 bp removed from the observed 15-mers [8]. We scanned the *N. denticulata* genome for the presence of exact matches to the 15-mer repeats, and alignment regions containing >100,000 counts were masked to prevent probe tiling across these regions [8]. Probes were tiled at 4x density across all sequences in each of the alignments from the 352 final AHE targets, and similar probes were removed. **Table S5** provides details of the target size and number of taxa representing each major lineage. The probes were divided across two Agilent SureSelect XT kits as follows: 1) Decapoda1a ELID=801331 containing Den1, Car1, and Ast1 (56698 probes total), and 2) Decapoda1b ELID=801341 containing Ach1, Ano1, and Bra1 (54854 probes total). The final probe sequences are available in the associated Dryad repository (https://doi.org/10.5061/dryad.k7505mn; subfolder D_Probe_design).

(e) AHE sequencing

Samples of 94 species (**Table S6**) were processed at the FSU Center for Anchored Phylogeny (www.anchoredphylogeny.com) following Lemmon et al. [1] and Prum et al. [2]. Briefly, DNA extracts passing QC by Qubit were sonicated to a size range of 200-500 bp using a Covaris E220 focused-ultrasonicator with Covaris microTUBES, and prepared to include single 8 bp library adapters. Libraries were pooled in groups of 16 and enriched using the aforementioned probes from the two Agilent SureSelect XT kits (probes from the two kits were pooled prior to the enrichment reaction). Enriched library pools of 16 samples were then pooled for sequencing such that each of two 48-sample pools were sequenced on an Illumina HiSeq2500 lane with a PE150 protocol and 8 bp indexing (85 Gb total).

(f) AHE QC and assembly

Preliminary investigations of the captured sequence data showed high variation across Decapoda in non-coding genomic regions outside of conserved exons, and third codon saturation within exons. Therefore we modified the exon-based AHE pipeline of Breinholt et al. [12] to allow for greater sequence divergence between taxa, and assembled the relatively conserved exons as our final loci for downstream phylogenomics.

Paired-end raw Illumina reads were cleaned using Trim Galore! v0.4.0 [17], allowing a minimum read size of 30 bp and trimming to remove bases with a Phred score below 20. To identify a reference set of single-copy exon loci for Iterative Baited Assembly (IBA; [12]) with the most coverage across decapod taxa, we used our AHE capture data and exon annotations from the published *Eriocheir sinensis* genome (Brachyura: Varunidae; [18]; NCBI PRJNA305216). We identified single-copy exons in the *E. sinensis* genome using single-hit and ortholog location genome mapping following Breinholt et al. ([12]; scripts: s_ hit_checker.py and ortholog_filter.py). These scripts identified exons that have either a single hit, or a second-best hit with a bit score <90% of the best hit to the reference genome; this process determines the best hit location of each captured AHE target to the reference genome, *E. sinensis* [12]. These single-copy exons from *E. sinensis* were screened against *de novo* Bridger assemblies of our cleaned AHE data (using default parameters: [19]) using the script genome_getprobe_TBLASTX.py (available: https://github.com/jessebreinholt/proteinIBA.git; [20]) that uses tblastx instead of blastn to identify sequences that resemble the single-copy exons, which were then screened for orthology using ortholog_filter.py [12].

A total of 675 exons that had 40% or more of the taxa sequenced for AHE samples in this study were used as the locus reference set called crab_ref1, which were translated into amino acids as bait for IBA. The 675 identified exon-based reference loci include nearly all exons that are represented in the 352 final AHE targets used in the probe design (key in Dryad). The number of exon-based reference loci in each of the 352 final AHE targets ranged from 1-15, with a mean of 3.4. Two exon-based reference loci were not found in the 352 final AHE target regions and are likely off-target or may flank one of the 352 final AHE target regions. The IBA successively uses USEARCH v7.0 [21] and Bridger v2014-12-01 [19] to assemble each locus in the reference set, and ensure it hits the targeted probe of the reference taxon (*E. sinensis*). IBA

was altered to take an amino acid reference using the script protein_IBA.py (available: https://github.com/jessebreinholt/proteinIBA.git). We assembled the set of 675 exon-based reference loci for each sequenced decapod taxon using protein_IBA with the k-mer size set to 25 and lower k-mer coverage of assembled sequences at 10x.

(g) Alignment, orthology, and alignment trimming

The IBA output, blast table and the assembled sequences for each exon-based locus were processed with protein_dir_fixer.py (available: https://github.com/jessebreinholt/proteinIBA.git). This script put all sequences in the same direction as the *E. sinensis* reference sequences, and trimmed them to match the probe region for ortholog screening. The sequences were queried using tblastx against the *E. sinensis* genome, and screened for orthology using the ortholog_filter.py following Breinholt et al. [12], which was used to parse blast tables and test if the top hit against the *E. sinensis* reference genome is at the same position of the target exon. As an alternative to the contamination screen used by Breinholt et al. [12], we used maximum kmer depth of the sequences assembled for each locus by selecting the sequences for every taxon with the lowest 'comp' number output by IBA. The lowest 'comp' number is the set of sequences and isoforms that received the greatest kmer depth in the Bridger assembly of each exon-based locus. This method provided results comparable to the contamination filter and removing duplicates step [12] without having to make assumptions about contamination using sequence similarity based on taxonomy. The full-length sequences of the inferred orthologs were aligned with MAFFT v7.245 [13]. As very little data appeared to be conserved or alignable across Decapoda in the introns flanking the exon region, we trimmed the sequence using the Extract_probe_region.py script [12]. Consensus of isoforms for each sequence were made to reduce to a single sequence per locus and taxon using FASconCAT-G v1.02 [22] following Breinholt et al. [12].

(h) Data matrix construction

The main data matrix comprised 410 exon-based loci (referred to throughout the manuscript), assembled with IBA, with at least 60% of the taxa represented in each locus. The average occupancy per locus = 81%; and completeness score as the total number of unambiguous characters divided by the size of the alignment = 80%. We processed the alignment of 410 exon-based loci with ALICUT/ALISCORE [23] to remove poorly aligned regions, but only three nucleotides were removed (and no amino acids) across all loci, thus this step was not included in the final dataset.A heatmap of pairwise amino acid completeness was constructed in ALISTAT [24] for a concatenated matrix of the 410 exon-based loci (**Figure S2**). Details of final amino acid and nucleotide matrices are described in **Table 2**.

(i) Systematic error

Systematic error is implicated in phylogenomics where the data violate assumptions of the model, leading to convergence of ever-larger datasets towards an incorrect topology with high support values (e.g. [25,26]). At the nucleotide level, both site-specific and lineage-specific biases can strongly influence phylogenetic results. We investigated site-specific biases (i.e.

multiple substitutions at the same site, or nucleotide saturation) by first building a saturation plot for each codon position with DAMBE v6 [27]. The saturation plot (**Figure S11**) indicated strong saturation of the third codon position, i.e. that this position evolved at a faster rate. Therefore, we conducted analyses on the full nucleotide set, as well as codons 1+2 only [28] as a form of data removal.

Broader biases in nucleotide compositional heterogeneity (lineage- and/or site-specific) were investigated using datasets that were recoded to exclude synonymous substitutions. These substitutions may or may not be saturated; biological base compositional bias is also accounted for. Recoding used ambiguity codes in the degen v1.4 Perl script [12,29]. Degen recoding does not change the matrix size; it merely reduces the degrees of freedom for possible substitution combinations.

In the amino acid dataset, site-specific amino acid biases may be accounted for with the CAT-GTR substitution model, but lineage-specific compositional biases do not have easily implementable models [30]. Therefore we adopted a similar approach as we did for nucleotides, using Dayhoff-6 recoding [30–32]. As with degen recoding, it does not change the matrix size, but groups the 20 amino acids into six classes that are similar on the basis of their biochemical properties, reducing the number of possible substitution combinations. This recoding strategy has been recommended for codon usage biases observed in pancrustacean nuclear genes in particular [32], though it has also been observed to collapse nodal support in other taxa e.g. [30,33].

(j) Phylogenetic analysis

For maximum likelihood (ML) analysis, PartitionFinder [34] on the 410 locus dataset (restricted to all versions of the LG model, including free rate models) obtained 149 best-fitting partitions. The best-fitting substitution models for each of the 149 partitions were selected in IQ-TREE v1.63 [35]. In IQ-TREE, 50 independent searches were run with different random seeds. All topologies were the same in each search, though branch lengths and scores differed. Support was assessed with 250 nonparametric bootstraps, with *a posteriori* convergence determined in RaxML using the MR, MRE, and MRE_IGN criteria (majority rule; convergence at 100) and FC criterion (frequency-based; convergence at 150). ML analyses were conducted on all matrices described in **Table 2**, except amino acid top 50.

For Bayesian inference, we used two chains and the CAT-GTR + G site-heterogeneous substitution model implemented in PhyloBayes v3.3f [36]. All Bayesian analyses were conducted on amino acid matrices; one matrix was recoded into the Dayhoff-6 functional groups. An automatic stopping rule was implemented, with tests of convergence every 100 cycles, until the default criteria of effective sizes and parameter discrepancies between chains were met (50 and 0.3, respectively), and with the bpcomp and tracecomp commands. Trees and posterior probability distributions were then generated from completed chains after the initial 20% of sampled generations were discarded as burn-in.

Coalescent (‘species tree’) methods were applied to investigate the role of incomplete lineage sorting e.g. [37,38]. ASTRAL is statistically consistent with the multispecies coalescent,

and can be effective if there are sufficient gene trees matching the ‘true’ tree [39]. As input, we used maximum likelihood gene trees calculated by IQ-TREE (only on amino acid data, otherwise as above) with SH-like support. The species tree was then estimated in ASTRAL-III v5.6.1 [40], collapsing nodes with <10% support, and estimating branch support using quartet node support (the percentage of quartets in gene trees that agree with a branch).

(k) Divergence time estimation

Divergence times were estimated in PhyloBayes v3.3f [36] using a fixed topology input based on the Bayesian CAT-GTR + G tree depicted in **Figure 2**. Preliminary runs indicated that the distant outgroups may exhibit heterotachy, so all outgroups were removed from this topology, except the two stomatopods. Due to the size of our data matrices and time to convergence, we used an amino acid alignment of only the top 50 loci; selection of these was based on the amino acid gene trees constructed for the ASTRAL analysis, with RaxML then used to calculate Robinson-Foulds statistics to compare each gene tree topology to the concatenated fixed topology [41]. Divergence time analysis was conducted in PhyloBayes under the CAT-GTR + G substitution model, and two runs of four chains. We compared the uncorrelated gamma multipliers (UGM) relaxed clock model [42], and the autocorrelated CIR model [43]. The root prior was defined based on the Eumalacostraca node [44], thus applying a gamma distribution with a mean of 440 Ma and SD of 20 Myr. All 19 internal fossil priors (justified in **Extended Data 2**) used soft bounds with 5% of the probability distribution allowed outside of the input ages, defined by a birth-death model [45]. An automatic stopping rule was implemented, with tests of convergence every 100 cycles, until the default criteria of effective sizes and parameter discrepancies between chains were met (50 and 0.3, respectively), and with the bpcomp and tracecomp commands. Trees and posterior probability distributions were then generated from completed chains after the initial 20% of sampled generations were discarded as burn-in. We also compared estimated posteriors to the truncated effective prior (by removing sequence data using the -prior flag in PhyloBayes; [46,47]; **Figure S13**).

2. Fossil Calibration Justifications:

We used 19 fossil calibrations, following the criteria of Parham et al. [48]. Node numbers listed below correspond to labels in **Figure 3**. A summary of fossils and their ages is provided in **Table S7**.

1. ***Node.*** This node comprises crown Verunipeltata ('Stomatopoda', or mantis shrimp) in our tree, with nomenclature as previously discussed [44,49], and monophyly matching Van Der Wal et al. [50]. All calibration data as in Wolfe et al. [44], node 51.

2. ***Node.*** This node represents crown Sergestoidea. In our phylogeny, this is the clade comprising *Lucifer*, *Parasergestes*, *Sergestes*, and *Deosergestes*, their last common ancestor and all of its descendants.

   Fossil specimens. *Paleomattea deliciosa* Maisey and Carvalho 1995 [51]. Holotype AMNH (American Museum of Natural History) 44985, carapace and abdominal segments dissolved from acid prep of teleost fossil.

   Phylogenetic justification. The phylogenetic position of this fossil was determined in a total evidence analysis [52]. It was found within crown Sergestoidea in their taxon sampling, sister taxon to *Acetes*. As it was outside of *Sergia* + *Deosergestes*, and we did not sample *Acetes*, we allow *P. deliciosa* to calibrate the clade including *Lucifer*. Note that a likely member of Luciferidae was recently discovered from the same deposits [53], and could be appropriate for this node as well.

   Age justification. Minimum as in Wolfe et al. [44], node 43. As the oldest decapod, *Palaeopalaemon newberryi* (node 6), is crownward of shrimps and prawns, a phylogenetic bracketing approach to obtain a soft maximum age for these groups is not appropriate. If we were to use a maximum age from the oldest crown Malacostraca, which would be 434.2 Ma [44], it would create priors that come into conflict with that of *P. newberryi* and its older age range for all decapods. Thus we conservatively adopt a soft maximum age of 521 Ma, as in node 1.

3. ***Node.*** This node represents crown Penaeoidea (penaeid shrimp/prawns). In our phylogeny it is the clade comprising Penaeidae, Sicyoniidae, Aristeidae, and Benthesicymidae, their last common ancestor and all of its descendants. Monophyly of this clade was also supported by a recent total evidence (morphology + three nuclear gene) phylogeny [52].

   Fossil specimens. *Ifasya madagascariensis* Van Straelen 1933 [54]. Several specimens examined for coding in Robalino et al. [52], including: MSNM (Museo di Storia Naturale di Milano, Milan, Italy) i11309, i9311, i9408, i14229, i9383, i9406, i9328, i11243, and i9328.

Phylogenetic justification. The phylogenetic position of this fossil was determined in a total evidence analysis [52]. It was found within crown Penaeidae, thus also crown Penaeoidea.

Age justification. *I. madagascariensis* was discovered in the Ambilobé region of northwest Magadascar [55,56]. The fossiliferous sediments bear the index conchostracan *Euestheria (Magniestheria) truempyi*, which may be correlated to the Bernburg Formation of Germany [57]. Although this correlation was used as an indicator of Olenekian age for Ambilobé [57], revisions to conchostracan biostratigraphy correlate *M. truempyi* to the Dienerian substage of the global Induan stage, Early Triassic [58]. The minimum age of the Induan (or the lower boundary of the Olenekian) is 251.2 Ma, based on the 2017 International Chronostratigraphic Chart, thus providing a minimum age for *I. madagascariensis*. Soft maximum as in node 2 herein.

4. ***Node.*** This node represents crown Stenopodidea (cleaner/boxer shrimp). In our phylogeny, this is the clade comprising the (currently recognized) genera *Stenopus*, *Microprosthema*, and *Macromaxillocaris*, their last common ancestor and all of its descendants.

   Fossil specimens. *Phoenice pasinii* Garassino 2001 [59]. Holotype, MSNM i24799.

   Phylogenetic justification. Recently, a need to revise the systematics of crown Stenopodidea has been identified based on a molecular phylogeny [60]. Only three fossil species have been described, and none have yet been evaluated using phylogenetics. Of these, two, *Devonostenopus pennsylvaniensis* Jones et al. 2014 [61] and *Jilinocaris chinensis* Schram et al. 2000 [62], were placed within Stenopodidea on characters that were admittedly poorly preserved and not conclusive. In contrast, *P. pasinii* is better preserved, and has a number of diagnostic characters confirming its stenopodidean affinity [59]. In particular, the subtriangular telson and presence of two longitudinal dorsal carinae on the uropodal endopods suggest a relationship to the Stenopodidae [59]. While it is not clear if *P. pasinii* belongs within crown versus stem Stenopodidae, it is reasonable to assign this fossil within crown Stenopodidea.

   Age justification. *P. pasinii* was discovered in the Hakel/Hâqel (holotype) and Hadjula/Hjoûla outcrops, northeast of Beirut, Lebanon [59]. Presence of the ammonite *Allocrioceras* cf. *annulatum* in the Hjoûla limestone correlates the deposit to the *Sciponoceras gracile* Zone in the Western Interior of the USA and the *Metoicoceras geslinianum* Zone globally [63]. The *S. gracile* Zone has a cyclostratigraphic minimum age of 94.39 Ma ± 0.12 Myr [64], providing a minimum age constraint of 94.27 Ma for *P. pasinii*. Soft maximum as in node 2 herein, to allow for the possibility that *Devonostenopus* is within the crown.

5. ***Node.*** This node represents crown Caridea. In our phylogeny, this clade is represented by Alpheidae (snapping shrimp), Atyidae (freshwater shrimp), Barbouriidae, Hippolytidae (cleaner and broken-back shrimp), Lysmatidae (cleaner and peppermint shrimp),

Oplophoridae (bioluminescent shrimp), Palaemonidae (freshwater and symbiotic anemone shrimp), and Thoridae (anemone shrimp), their last common ancestor and all of its descendants. Based on previous molecular trees, and our topology, Procarididea (anchialine shrimp) are excluded from the otherwise monophyletic crown Caridea [65]. Although we did not sequence Amphionidacea, recent analysis of four genes [66] placed this organism as a suspected larval pseudo-taxon within our concept of Caridea, thus the calibration node would not need to be modified if they are added in future.

Fossil specimens. *Blaculla haugi* Winkler 2015 [67], holotype SMNS (Staatliches Museum für Naturkunde, Stuttgart, Germany) 70286.

Phylogenetic justification. *B. haugi* is within crown Caridea based on overlap of the pleonal pleurae, and the first two pereiopods being chelate while the third, fourth, and fifth are achelate [67]. The first two pereiopods have some characteristics in common with the extant clade ‘Alpheoidea’ (see below), with stouter first pereiopods and multi-jointed second pereiopods [67]. However, pereiopod appendage morphology across caridean families appears to be convergent [68], which challenges the ability to correctly assign fossils to crown families based on these morphologies (also challenging the confidence in older putative caridean fossils). Mandibular structure is possibly more diagnostic [68], however, mouthparts are not well preserved in Solnhofen material [67]. Furthermore, the assumed composition of crown Alpheoidea does not include Palaemonidae [69,70], but these are found within a paraphyletic group within our tree (also supported in previous molecular trees: [71,72]). Additional putative caridean fossils are also known from the Solnhofen limestones, e.g. [73–75], and are thus of the same age, suggesting Caridea had begun to diversify. We remain agnostic on proposed, but not diagnostic, caridean fossils from the Early Triassic Paris Biota of Idaho [76]. The several possible Solnhofen taxa, together with the morphology of *B. haugi*, permit a conservative minimum age constraint on crown Caridea in its entirety, rather than on any specific families.

Age justification. The fossil of *B. haugi* was found in the Solnhofen Plattenkalk (lithographic limestone) of Eichstätt, Bavaria, Germany [67]. As discussed by Benton et al. ([77], node 31), a minimum age for Solnhofen fossils is 150.94 Ma. Soft maximum as in node 2 herein.

6. ***Node.*** This node represents crown Reptantia. In our phylogeny, this is the clade comprising Axiidea, Astacidea, Achelata, Polychelida, Gebiidea, Anomura, and Brachyura, their last common ancestor and all of its descendants. Glypheidea are included in previous formulations of Reptantia, and if corroborated by future phylogenomic data (as already suggested in the mitogenome tree of Tan et al. [78]), they will not affect our calibration choice. As in the discussion of Wolfe et al. [44] node 49, the Devonian fossil *Palaeopalaemon newberryi* Whitfield 1880 [79] is within crown Reptantia. This is implicitly confirmed in the phylogenetic analysis of Jones et al. [80]. Thus all calibration data including both age priors as in Wolfe et al. [44], nodes 49, 55, and 56.

7. ***Node.*** This node represents crown Achelata, a clade comprising the families Palinuridae (spiny lobsters) and Scyllaridae (slipper lobsters), their last common ancestor and all of its descendants.

   Fossil specimens. *Yunnanopalinura schrami* Feldmann et al. 2012 [81]. Holotype LPI (Luoping section, Invertebrate Paleontology Collection, Chengdu Institute of Geology and Mineral Resources) 40169.

   Phylogenetic justification. This species has been previously justified as a calibration for Achelata [81,82].

   Age justification. *Y. schrami* was recovered from limestone of the Luoping Biota, Member II of the Guanling Formation, near Luoping, Yunnan, south China [81,83]. Extensive stratigraphy of the Luoping biota places the Guanling Formation just below the uppermost boundary of the Anisian stage [83]. The upper boundary of the Anisian is estimated at 241.5 Ma ± 1 Myr [58], thus providing a minimum age at 240.5 Ma. A soft maximum age is obtained by phylogenetic bracketing, with the generous assumption that crown Achelata are not older than the oldest known crown Decapoda, which is *Palaeopalaemon newberryi* [44]. The age of the Chagrin Shale, which bears *P. newberryi*, is late Fammenian based on the presence of index algae; there is no lower bound index fossil mentioned [44]. Thus a maximum age of this deposit is estimated as the lower bound of the Fammenian, at 372.2 Ma [84].

8. ***Node.*** This node represents crown Nephropidae (true lobsters). In our tree, this includes *Thaumastocheles*, *Nephropoides*, and *Nephropsis*, their last common ancestor and all of its descendants. Note that the family Thaumastochelidae is now synonymized with Nephropidae [85].

   Fossil specimens. *Jagtia kunradensis* Tshudy & Sorhannus 2000 [86]. Holotype IRScNB (Institut Royal des Sciences Naturelles de Belgique, Brussels) 90-33h.

   Phylogenetic justification. Morphological phylogenetic analysis places *J. kunradensis* as more closely related to *Nephropsis* and *Nephropoides* than to *Thaumastocheles* [87]. Thus *J. kunradensis* is in the crown group. Another lobster fossil (*Oncopareia*) within the crown group in this analysis was not referred to specific material, and is of similar age to *J. kunradensis*. *Hoploparia stokesi* was also found within the crown group Nephropidae by Karasawa et al. [87], but the systematics of this genus demand revision [88]. Such revisions would likely compromise the wider stratigraphic range reported for *Hoploparia* [89]. Thus *J. kunradensis* is the most conservative calibration fossil for Nephropidae.

   Age justification. *J. kunradensis* has been collected from the Kunrade Limestone facies of the Maastricht Formation, southeast Netherlands [86]. The Maastricht Formation is eponymous for the Maastrichtian stage of the latest Cretaceous (although it does not bear the GSSP for either lower or upper stage boundary; [64]). The upper boundary of the Maastrichtian is well constrained at 66.0 Ma [90], thus providing a minimum age for

Nephropidae. Soft maximum as in node 8 herein.

9. ***Node.*** This clade, in our tree, comprises Cambaridae, Cambaroididae, Astacidae, and Parastacidae (together: crayfish), their last common ancestor and all of its descendants. Monophyly of freshwater crayfishes has been previously established by a number of molecular and morphological analyses, e.g. [82,91].

   Fossil specimens. *Cricoidoscelosus aethus* Taylor et al. 1999 [92]. Based on holotype NIGP (Nanjing Institute of Geology and Palaeontology) 126337 and NIGP 126355 [87].

   Phylogenetic justification. Morphological phylogenetic analysis places *C. aethus* as the sister of a clade comprising the extant crayfish *Cambarus* and *Procambarus*, both members of Cambaridae [87]. The published morphological tree places *C. aethus* further crownward than Parastacidae [87], in relationships that mirror our AHE topology. Therefore, it is an appropriate fossil to calibrate the freshwater crayfish crown group.

   Age justification. Minimum as in Wolfe et al. [44], node 60. Soft maximum as in node 8 herein.

10. ***Node.*** This node represents crown Axiidea (mud shrimp/ghost shrimp). In our tree, this clade is represented by Axiidae, Callianassidae, Callianideidae, Gourretiidae, their last common ancestor and all of its descendants. Monophyly of this clade is established by molecular phylogeny of the 16S, 28S, and 18S genes [93,94].

    Fossil specimens. *Protaxius isochela* Woodward 1876 [95]. Calibration material is from specimens MAN (Museum-Aquarium at Nancy, France) 11700-11762 [96].

    Phylogenetic justification. As discussed by Hyžný & Klompmaker [97], the fossil record of mud shrimps usually preserves only the distal cheliped elements, and many are assumed to be members of a wastebasket ‘*Callianassa*’, which compromises systematic identification. The oldest putative members are Jurassic, all of which are likely most closely related to crown Axiidae [97]. The very oldest, *Magila bonjouri* Étallon 1861, was described from a preserved dactylus + propodus, but the holotype cannot be found [97]. The only Jurassic species with full body preservation is *P. isochela*, where the specimen figured (drawn) by Woodward is unfortunately not identified ([97], supplement). However, Hyžný & Klompmaker [97] mention material of *P. isochela* from France as accepted within this taxon, thus we may calibrate a minimum age from the specimens discussed by Breton et al. [96]. Although the relationship of *P. isochela* to crown Axiidae is not precisely known, it is well within the crown-group of Axiidea.

    Age justification. French *P. isochela* material was recovered from wells at Bure, Meuse, in the northeast of France [96]. The locality belongs to the *Rasenia cymodoce* to *Aulacostephanus mutabilis* ammonite Zone [96]. The upper boundary of the *A. mutabilis* Zone is Chron M23r.2r.1, with an age of 153.55 Ma [98], in the Kimmeridgian. This provides a minimum age estimate for Axiidea. Soft maximum as in node 8 herein.

11. ***Node.*** This node represents crown Gebiidea (mud shrimp/mud lobster/ghost shrimp). In our tree, this is only represented by Laomediidae and Axianassidae, their last common ancestor and all of its descendants.

    Fossil specimens. *Laurentiella imaizumii* Karasawa 1993 [99]. Material figured by Karasawa [99] includes MFM (Mizunami Fossil Museum, Mizunami, Gifu Prefecture, Japan) 39003-39006, and MFM 39117.

    Phylogenetic justification. Based on molecular phylogenetics, Laomediidae and Axianassidae are sister clades within Gebiidea, exclusive of the clades we did not sample: Thalassinidae and Upogebiidae [93,94]. No fossil Axianassidae are recorded, thus we must calibrate based on fossil Laomediidae. While the position of *L. imaizumii* within either the crown or stem of Laomediidae is unknown, it does share characters indicating its membership within the total group of Laomediidae (e.g. strongly heterochelate chelipeds; [99]). Thus, *L. imaizumii* is within the crown group of the represented Gebiidea. Note that the extant genus *Laurentiella* is considered a junior homonym of *Saintlaurentiella* [100]; this does not influence the calibration choice.

    Age justification. The oldest occurrence of *L. imaizumii* is in the Akeyo Formation of the Mizunami Group, Gifu Prefecture, Japan [99,101]. The type locality, the Toyoda Formation, is slightly younger [99,102]. Thus we calibrate based on the Akeyo Formation, which is the uppermost member of the Mizunami Group, and correlated to the C5Dr chron based on diatom fossils [101]. Globally, these strata underlie the correlated NMU 5 (Asia) and MN 5 (Europe) units. Thus a conservative upper bound age for the Akeyo Formation is 17 Ma. Soft maximum as in node 8 herein.

12. ***Node.*** This clade, in our tree, comprises Porcellanidae (porcelain crabs) and Munididae (some squat lobsters), their last common ancestor and all of its descendants. Based on previous total evidence analysis [103], these families are close relatives. The full breadth of Galatheoidea are not represented here.

    Fossil specimens. *Juracrista perculta* Robins et al. 2012 [104]. Holotype NHMW 2007z0149/036 (Natural History Museum of Vienna) and paratypes NHMW 2007z0149/0370 and NHMW 2007z0149/0371.

    Phylogenetic justification. *J. perculta* is known from dorsal carapace material, and was previously used to calibrate Munididae [103]. Its carapace exhibits pronounced supraorbital spines and broad rostral shape, which typify Munididae [104]. This fossil differs from Galatheidae and Munidopsidae in its possession of transverse ornamentation without a triangular rostrum (preservation of the rostrum is rare and diagnostic) [104]. The breadth of the rostrum in *J. perculta* is larger than extant munidids, suggesting a close relationship but perhaps indeterminate whether it is in the crown group. Therefore *J. perculta* is at the least, a member of the total group of Munididae, and thus belongs within the crown group of Porcellanidae + Munididae. Putative members of Munidopsidae [105] and Porcellanidae [106] were also discovered in the Ernstbrunn Limestone, although the porcellanid awaits a major revision (A. Klompmaker, pers.

comm.). These discoveries further support divergence of the major Galatheoidea lineages prior to the Cretaceous.

Age justification. *J. perculta* was recovered from the Ernstbrunn Limestone, lower Austria [104]. Ammonites are unavailable for precise biostratigraphy from this locality, but a nearby locality from the same unit preserves the ammonites *Richterella richteri*, *Simplisphinctes*, and the diagnostic *Micracanthoceras microcanthum* constraint for the late Tithonian [98,107]. However, benthic foraminifera and calcareous algae suggest the Ernstbrunn Limestone may have been deposited as late as the early Cretaceous, early Berriasian stage [108]. Although most literature accepts a Tithonian age, we recognize that the more conservative constraint should allow some probability density in the early Berriasian, which has a minimum age of approximately 142 Ma [98]. A soft maximum age is obtained by phylogenetic bracketing, with the generous assumption that crown Porcellanidae + Munididae are not older than the oldest putative crown Anomura. Previous studies have suggested the oldest Anomura is *Platykotta akaina* [103,109]. However, its second pair of chelate pereiopods makes this affinity uncertain and it could even be stem-group Meiura [110]; nevertheless, *P. akaina* is surely older than crown Porcellanidae + Munididae. *P. akaina* was collected at Wadi Naqab close to Ras Al Khaimah City, United Arab Emirates, from limestone of the Ghalilah Formation [109]. No precise constraint is available, so a soft maximum age is the base of the Norian stage, at ~227 Ma.

13. ***Node.*** This node represents crown Paguroidea (hermit and king crabs). In our tree, this includes Coenobitidae, Diogenidae, Paguridae, Lithodidae, their last common ancestor and all of its descendants. Our AHE results follow the topology of the Bayesian molecular-only analysis of Bracken-Grissom et al. ([103], their Figure 2) in excluding Parapaguridae from a monophyletic Paguroidea.

    Fossil specimens. *Diogenicheles theodorae* Fraaije et al. 2012 [111]. Holotype I−F/MP/3957/1533/08 (Institute of Systematics and Evolution of Animals, Polish Academy of Sciences, Kraków, Poland).

    Phylogenetic justification. The assignment of *D. theodorae* to crown Paguroidea is based on carapace material, and was justified in Bracken-Grissom et al. [103]. It bears similarities (a distinct threefold junction of keraial, massetic and anterior branchial areas of the outer carapace) with the family Parapylochelidae, which is likely closely related to the other symmetrical hermit crabs in Pylochelidae [111]. The total evidence phylogeny of Bracken-Grissom et al. [103] places Pylochelidae as the most deeply branching lineage within Paguroidea.

    Age justification. *D. theodorae* was discovered in an abandoned quarry in Bzów, southern Poland [111]. As discussed by Fraaije et al. [111], this locality preserves the ammonites *Ochetoceras canaliculatum*, *Trimarginites trimarginatus*, *Dichotomosphinctes* sp., and *Glochioceras subclausum*. Together, these ammonites are globally correlated to the *Gregoriceras transversarium* ammonite Zone of the Oxfordian.

Cyclo- and magnetostratigraphy indicate a minimum age of 159.44 Ma [98] for the *G. transversarium* Zone, and thus for *D. theodorae*. Soft maximum as in node 13 herein.

14. ***Node.*** This clade, in our tree, comprises Paguridae (hermit crabs) and Lithodidae (king crabs), their last common ancestor and all of its descendants.

    Fossil specimens. *Paralithodes bishuensis* Karasawa et al. 2017 [112]. Holotype MFM 83077.

    Phylogenetic justification. No phylogenetic analysis has yet been conducted to evaluate the relationships among extant and fossil pagurids, and the taxonomy of fossil members remains problematic [113]. As Paguridae is paraphyletic with respect to Lithodidae in previous molecular and total evidence analyses [103,114], fossils that may be within Paguridae are not guaranteed to fall within this node (as they may be members of lineages leading to pagurids that are outside of our AHE taxon sampling). Therefore we conservatively use the oldest likely fossil of Lithodidae. *P. bishuensis* possesses several diagnostic features allying it with members of the extant genus *Paralithodes*, particularly the sparsely arranged low, pointed dorsal tubercles on the carapace [112]. Thus, a position within crown Lithodidae is confirmed. Although previous publications have suggested the oldest Lithodidae is *Paralomis debodeorum* Feldmann 1998 [115], the sediments in which it is found are poorly constrained and may be as young as the Pliocene.

    Age justification. The type locality for *P. bishuensis* is ‘locality MRZ06’, Minamichita-cho, Aichi Prefecture, Japan, found in sandstone of the Yamami Formation of the Morozaki Group [112]. Biostratigraphic index fossils include the diatom *Crucidenticula sawamurae*, which is correlated in North America to the C5Cn chron, ECDZ2, and *Delphineis ovata* Zone [116]. The approximate age of the top of the ECDZ2 is 15.8 Ma [116], providing a minimum age constraint. Soft maximum as in node 13 herein.

15. ***Node.*** This node represents crown Eubrachyura (‘higher’ true crabs). In our tree, this includes Heterotremata and Thoracotremata, their last common ancestor and all of its descendants. Monophyly of Eubrachyura has been supported in previous molecular analyses [117].

    Fossil specimens. *Telamonocarcinus antiquus* Luque 2015 [118]. Holotype IGM (Colombian Geological Survey, Bogotá, Colombia) p881012.

    Phylogenetic justification. The phylogenetic position of *T. antiquus* within Eubrachyura is based on characters shared with extant Dorippoidea (i.e. Dorippidae and Ethusidae). While the position of gonopores is unclear [118], preventing definitive assignment to Heterotremata, the distinctive carapace outline and groove pattern in particular ally this fossil with crown Dorippoidea. Luque [118] concluded that Dorippoidea may be an early branching lineage of Eubrachyura. Although no members of Dorippidae or Ethusidae were included in our AHE sampling, their closest relative in a previous molecular phylogeny was Leucosiidae [117], which we did include. Given the uncertainty in the

fossil's possession of the defining character of Heterotremata (male coxal gonopores), and the exact position of Dorippoidea, we conservatively calibrate only the Eubrachyura using *T. antiquus*.

Age justification. The fossil of *T. antiquus* was discovered from shales of the lowermost Tablazo Formation, in El Batán, Montegrande, near the town of La Fuente, Department of Santander, Colombia [118]. The Tablazo Formation bears *Parahoplites* and *Douvilleiceras* ammonites, and locally is within the *Douvilleiceras solitae–Neodeshayesites columbianus* Zone [118]. Globally, *Douvilleiceras mammillatum* straddles the early to middle Albian [64]. The *D. mammillatum* Zone thus provides a conservative minimum age for *T. antiquus* at 110.22 Ma [64]. A soft maximum age is obtained by phylogenetic bracketing, with the generous assumption that crown Eubrachyura are not older than the oldest crown Brachyura. The oldest crown Brachyura is debatable; *Eocarcinus praecursor* [119] and *Eoprosopon klugi* [120] have both been proposed, but both lack some crown characters and are only represented by rather poorly preserved dorsal carapaces [110]. Nevertheless, stem-lineage positions of these taxa would imply the Brachyura crown may be even younger, so we calibrate the soft maximum from the base of the Pliensbachian, at 191.8 Ma.

16. ***Node.*** This node represents crown Thoracotremata. In our tree, this clade is comprised of the sampled families Grapsidae (marsh/shore crabs), Ocypodidae (ghost and fiddler crabs), Plagusiidae, Sesarmidae, and Varunidae, their last common ancestor and all of its descendants. Monophyly of Thoracotremata is supported by male gonopores located on the sternum, and by previous molecular phylogenies [117]. Monophyly of previously discussed superfamilies (e.g. Grapsoidea, Ocypodidea) is under suspicion from this and other molecular phylogenies [117,121], so the clade treated herein remains Thoracotremata.

    Fossil specimens. *Litograpsus parvus* Müller & Collins 1991 [122] (as revised by Schweitzer & Karasawa 2004 [123]), holotype M.91-227 (Natural History Museum of Hungary).

    Phylogenetic justification. Members of Thoracotremata are rare and hard to identify in the fossil record, likely because many live in difficult to preserve intertidal and semi-terrestrial habitats. *L. parvus* shares characters with extant Grapsidae and Sesarmidae, such as the rectangular carapace, size and positioning of the orbits, and a transverse ridge formed by the cardiac region with broad branchial ridges [123]. Although the exact relationship to the extant members is unknown, based on our topology, a position of *L. parvus* on the stem of either Grapsidae or Sesarmidae would still be within crown-group Thoracotremata. Although without sufficient confirmation, some older crown-group fossils most likely exist for Thoracotremata. There is a possible 'grapsoid' crab from mid-late Paleocene sediments of Colombia (Luque et al. 2017 [124], Fig. 8J), but it has not yet received systematic study. Possible stem-group 'Pinnotheridae' fossils *Viapinnixa alvarezi* and *V. perrilliatae* are known from the early Eocene (Ypresian; [125,126]) of Chiapas, Mexico; however Pinnotheridae are not sampled here, and at least some

members may fall outside of the crown-group we define [117,127–129]. Finally, limb fragments of *Varuna*? sp. have been reported from the middle Eocene (Lutetian?) of Jamaica [124,130,131], but with limited specimen or stratigraphic information.

Age justification. *L. parvus* is known from limestone sediments of the Szépvölgy Formation, Hungary [122]. Co-occurring foraminifera constrain the age of the Szépvölgy Limestone to the NP20 zone of the C15n chron [122,132]. This is Priabonian, with an upper boundary of 33.9 Ma, providing a minimum age constraint. Soft maximum as in node 16 herein.

17. ***Node.*** This node represents crown Heterotremata. In our tree, this clade is comprised of the sampled families Atelecyclidae, Bellidae, Corystidae, Leucosiidae (purse crabs), Menippidae (stone crabs), Platyxanthidae, and the superfamilies Portunoidea (swimming crabs), Xanthoidea (mud crabs) and Majoidea (spider and decorator crabs), their last common ancestor and all of its descendants. Composition of Portunoidea as in Evans [133]. Compositions of Xanthoidea and Majoidea are as defined in the molecular analysis of Tsang et al. [117], although monophyly of their constituent families remains questionable.

    Fossil specimens. *Cretamaja granulata* Klompmaker 2013 [134]. Holotype MGSB (Museo Geológico del Seminario de Barcelona, Spain) 77706A+B.

    Phylogenetic justification. Klompmaker [134] diagnosed *Cretamaja* as appropriately belonging to Majoidea based on carapace shape (which exhibits rampant convergence among brachyurans) and presence of anterolateral spines. These characters (especially because of the limitations of carapace shape) only permit assignment to a deeply divergent lineage of Majoidea, however, likely outside the Majoidea crown group [117]. While monophyly of Majoidea has been supported by previous molecular and morphological phylogenies [117,135–137], the exact relationships among constituent families (in our tree, Epialtidae, Inachoididae, and Mithracidae) are debated. A position for *C. granulata* along the stem of Majoidea would still permit assignment to the crown group of Heterotremata, and thus a calibration of the latter clade.

    Age justification. The Koskobilo fauna belongs to the Albinez Unit of the Eguino Formation, southwest of Alsasua, Spain [134]. Either a Cenomanian or late Albian age has been discussed for the Ablinez Unit, based on underlying ammonites and those of contemporaneous reef deposits (summarized by Klompmaker [134]). *Mortoniceras perinflatum* was one of the contemporaneous ammonites from a nearby locality, and it is an index fossil for the late Albian [64], a convincing age. The upper boundary of the *M. perinflatum* Zone is at 100.91 Ma [64], which is therefore the minimum age of *C. granulata*. Soft maximum as in node 16 herein.

18. ***Node.*** This node represents crown Majoidea (spider and decorator crabs). In our tree, this clade includes Epialtidae, Inachoididae, and Mithracidae, their last common ancestor and all of its descendants. While monophyly of Majoidea has been supported by previous

molecular and morphological phylogenies [117,135–137], the exact relationships among constituent families are debated.

Fossil specimens. *Planobranchia palmuelleri* Artal et al. 2014 [138]. Holotype MGSB 79782.

Phylogenetic justification. The most distinctive characters for majoids are the carapace shape. *P. palmuelleri* has an advanced carapace front with straight lateral margins, rounded longitudinal frontal ridges, lateral orbits with a strong outer-orbital subtriangular tooth, and dorsal conical spines: these characters refer *Planobranchia* to the Inachidae. Membership on the stem-lineage of Inachidae tentatively confirms the ability to provide a minimum calibration for the crown Majoidea we have sampled. Late Cretaceous [124,139], Eocene [140,141], and Oligocene [142] putative majoids have been discovered with preserved carapaces, but they either fall outside of our molecular crown taxon sampling, or lack specimen information.

Age justification. *P. palmuelleri* is known from strata of the Vic area, Barcelona province, Catalonia, Spain, most likely assigned to the Coll de Malla Formation [138]. As there is some controversy over the precise lithostratigraphic unit [143], we agree with Artal et al. [138] that a Lutetian age is conservatively appropriate. The upper bound of the Lutetian is 41.2 Ma, providing a minimum age. Soft maximum as in node 16 herein.

19. ***Node.*** This node represents crown Xanthoidea (mud crabs). In our tree, the members are ‘Xanthidae’ and Panopeidae, their last common ancestor and all of its descendants. Monophyly of a clade containing at least these members of Xanthoidea is supported by previous molecular and total evidence phylogenies [117,144].

    Fossil specimens. *Phlyctenodes tuberculosus* Milne Edwards 1862 [145]. The holotype MNHN (Muséum National d’Histoire Naturelle, Paris) R03826, and specimen MCZ (Museum of Comparative Zoology, Harvard University) 2456 are figured by Busulini et al. [146].

    Phylogenetic justification. *Phlyctenodes* fossils are only known from carapaces, which are linked with members of the xanthid subfamily Actaeinae based on the ornamentation of the carapace with tubercles [146,147]. However, as many of the subfamilies within Xanthidae, including Actaeinae, are very likely polyphyletic [144,148], and even our focal analysis suggests that Xanthidae may be paraphyletic, the exact relationship of *P. tuberculosus* to sampled taxa is unclear. Thus we calibrate the crown group of all of sampled Xanthoidea. Of contemporaneous Xanthoidea fossils [147], *P. tuberculosus* has recently refigured and discussed specimens, and is thus selected.

    Age justification. The holotype of *P. tuberculosus* was attributed to the locality Hastingues, Landes, France, in the ‘middle Eocene’ [146]. The MCZ specimen was discovered in the better known San Feliciano Hill quarry of the Berici Hills, Vicenza, Italy [146]. The decapod-bearing strata of the quarry are correlated to the lower Priabonian stage, late Eocene, based on calcareous nannofossils [149,150]. The upper

boundary of the Priabonian is 33.9 Ma, providing a minimum age constraint. Soft maximum as in node 16 herein.

3. Extended References:

1. Lemmon AR, Emme SA, Lemmon EM. 2012 Anchored Hybrid Enrichment for Massively High-Throughput Phylogenomics. *Systematic Biology* **61**, 727–744.
2. Prum RO, Berv JS, Dornburg A, Field DJ, Townsend JP, Lemmon EM, Lemmon AR. 2015 A comprehensive phylogeny of birds (Aves) using targeted next-generation DNA sequencing. *Nature* **526**, 569–573.
3. Rokyta DR, Lemmon AR, Margres MJ, Aronow K. 2012 The venom-gland transcriptome of the eastern diamondback rattlesnake (*Crotalus adamanteus*). *BMC Genomics* **13**, 312.
4. Alexandrou MA *et al.* 2015 Evolutionary relatedness does not predict competition and co-occurrence in natural or experimental communities of green algae. *Proceedings of the Royal Society B: Biological Sciences* **282**, 20141745.
5. Grabherr MG *et al.* 2011 Full-length transcriptome assembly from RNA-Seq data without a reference genome. *Nature Biotechnology* **29**, 644–652.
6. Zheng Y, Zhao L, Gao J, Fei Z. 2011 iAssembler: a package for *de novo* assembly of Roche-454/Sanger transcriptome sequences. *BMC Bioinformatics* **12**, 453.
7. Young AD *et al.* 2016 Anchored enrichment dataset for true flies (order Diptera) reveals insights into the phylogeny of flower flies (family Syrphidae). *BMC Evolutionary Biology* **16**, 143.
8. Hamilton CA, Lemmon AR, Lemmon EM, Bond JE. 2016 Expanding anchored hybrid enrichment to resolve both deep and shallow relationships within the spider tree of life. *BMC Evolutionary Biology* **16**, 212.
9. Dietrich CH *et al.* 2017 Anchored Hybrid Enrichment-Based Phylogenomics of Leafhoppers and Treehoppers (Hemiptera: Cicadomorpha: Membracoidea). *Insect Systematics and Diversity* **1**, 57–72.
10. Haddad S, Shin S, Lemmon AR, Lemmon EM, Svacha P, Farrell B, Ślipiński A, Windsor D, McKenna DD. 2018 Anchored hybrid enrichment provides new insights into the phylogeny and evolution of longhorned beetles (Cerambycidae). *Systematic Entomology* **43**, 68-89.
11. Winterton SL *et al.* 2017 Evolution of lacewings and allied orders using anchored phylogenomics (Neuroptera, Megaloptera, Raphidioptera). *Systematic Entomology.*
12. Breinholt JW, Earl C, Lemmon AR, Lemmon EM, Xiao L, Kawahara AY. 2018 Resolving relationships among the megadiverse butterflies and moths with a novel pipeline for Anchored Phylogenomics. *Systematic Biology* **67**, 78–93.
13. Katoh K, Standley DM. 2013 MAFFT Multiple Sequence Alignment Software Version 7: Improvements in Performance and Usability. *Molecular Biology and Evolution* **30**, 772–780.
14. Kearse M *et al.* 2012 Geneious Basic: An integrated and extendable desktop software platform for the organization and analysis of sequence data. *Bioinformatics* **28**, 1647–1649.
15. Tan MH, Gan HM, Gan HY, Lee YP, Croft LJ, Schultz MB, Miller AD, Austin CM. 2016 First comprehensive multi-tissue transcriptome of *Cherax quadricarinatus* (Decapoda: Parastacidae) reveals unexpected diversity of endogenous cellulase. *Organisms Diversity & Evolution* **16**, 185–200.
16. Kenny N *et al.* 2014 Genomic Sequence and Experimental Tractability of a New Decapod Shrimp Model, *Neocaridina denticulata*. *Marine Drugs* **12**, 1419–1437.

17. Krueger F. 2015 *Trim Galore. A wrapper tool around Cutadapt and FastQC to consistently apply quality and adapter trimming to FastQ files*. See www.bioinformatics.babraham.ac.uk/projects/trim_galore/.
18. Song L *et al.* 2016 Draft genome of the Chinese mitten crab, *Eriocheir sinensis*. *GigaScience* **5**, 5.
19. Chang Z, Li G, Liu J, Zhang Y, Ashby C, Liu D, Cramer CL, Huang X. 2015 Bridger: a new framework for *de novo* transcriptome assembly using RNA-seq data. *Genome Biology* **16**, 30.
20. Espeland M *et al.* 2018 A Comprehensive and Dated Phylogenomic Analysis of Butterflies. *Current Biology* **28**, 770-778.e5.
21. Edgar RC. 2010 Search and clustering orders of magnitude faster than BLAST. *Bioinformatics* **26**, 2460–2461.
22. Kück P, Meusemann K. 2010 FASconCAT: Convenient handling of data matrices. *Molecular Phylogenetics and Evolution* **56**, 1115–1118.
23. Kück P, Meusemann K, Dambach J, Thormann B, von Reumont BM, Wägele JW, Misof B. 2010 Parametric and non-parametric masking of randomness in sequence alignments can be improved and leads to better resolved trees. *Frontiers in Zoology* **7**, 10.
24. Misof B *et al.* 2014 Phylogenomics resolves the timing and pattern of insect evolution. *Science* **346**, 763–767.
25. Kocot KM *et al.* 2017 Phylogenomics of Lophotrochozoa with consideration of systematic error. *Systematic Biology* **66**, 256-282.
26. Philippe H, Vienne DM de, Ranwez V, Roure B, Baurain D, Delsuc F. 2017 Pitfalls in supermatrix phylogenomics. *European Journal of Taxonomy.*
27. Xia X, Xie Z, Salemi M, Chen L, Wang Y. 2003 An index of substitution saturation and its application. *Molecular Phylogenetics and Evolution* , 7.
28. Breinholt JW, Kawahara AY. 2013 Phylotranscriptomics: Saturated Third Codon Positions Radically Influence the Estimation of Trees Based on Next-Gen Data. *Genome Biology and Evolution* **5**, 2082–2092.
29. Zwick A, Regier JC, Zwickl DJ. 2012 Resolving Discrepancy between Nucleotides and Amino Acids in Deep-Level Arthropod Phylogenomics: Differentiating Serine Codons in 21-Amino-Acid Models. *PLoS ONE* **7**, e47450.
30. Feuda R, Dohrmann M, Pett W, Philippe H, Rota-Stabelli O, Lartillot N, Wörheide G, Pisani D. 2017 Improved Modeling of Compositional Heterogeneity Supports Sponges as Sister to All Other Animals. *Current Biology* **27**, 3864-3870.e4.
31. Susko E, Roger AJ. 2007 On Reduced Amino Acid Alphabets for Phylogenetic Inference. *Molecular Biology and Evolution* **24**, 2139–2150.
32. Rota-Stabelli O, Lartillot N, Philippe H, Pisani D. 2013 Serine codon-usage bias in deep phylogenomics: Pancrustacean relationships as a case study. *Systematic Biology* **62**, 121–133.
33. Laumer CE. 2018 Inferring ancient relationships with genomic data: a commentary on current practices. *Integrative and Comparative Biology* **58**, 623–639.
34. Lanfear R, Calcott B, Ho SYW, Guindon S. 2012 PartitionFinder: Combined Selection of Partitioning Schemes and Substitution Models for Phylogenetic Analyses. *Molecular Biology and Evolution* **29**, 1695–1701.

35. Nguyen L-T, Schmidt HA, von Haeseler A, Minh BQ. 2015 IQ-TREE: A Fast and Effective Stochastic Algorithm for Estimating Maximum-Likelihood Phylogenies. *Molecular Biology and Evolution* **32**, 268–274.
36. Lartillot N, Rodrigue N, Stubbs D, Richer J. 2013 PhyloBayes MPI: Phylogenetic Reconstruction with Infinite Mixtures of Profiles in a Parallel Environment. *Systematic Biology* **62**, 611–615.
37. Edwards SV. 2009 Is a new and general theory of molecular systematics emerging? *Evolution* **63**, 1–19.
38. Edwards SV *et al.* 2016 Implementing and testing the multispecies coalescent model: A valuable paradigm for phylogenomics. *Molecular Phylogenetics and Evolution* **94**, 447–462.
39. Mirarab S, Warnow T. 2015 ASTRAL-II: coalescent-based species tree estimation with many hundreds of taxa and thousands of genes. *Bioinformatics* **31**, i44–i52.
40. Zhang C, Sayyari E, Mirarab S. 2017 ASTRAL-III: Increased Scalability and Impacts of Contracting Low Support Branches. In *RECOMB International Workshop on Comparative Genomics*, pp. 53–75. Cham, Switzerland: Springer.
41. Smith SA, Brown JW, Walker JF. 2018 So many genes, so little time: A practical approach to divergence-time estimation in the genomic era. *PLOS ONE* **13**, e0197433.
42. Drummond AJ, Ho SYW, Phillips MJ, Rambaut A. 2006 Relaxed Phylogenetics and Dating with Confidence. *PLoS Biology* **4**, e88.
43. Lepage T, Bryant D, Philippe H, Lartillot N. 2007 A General Comparison of Relaxed Molecular Clock Models. *Molecular Biology and Evolution* **24**, 2669–2680.
44. Wolfe JM, Daley AC, Legg DA, Edgecombe GD. 2016 Fossil calibrations for the arthropod Tree of Life. *Earth-Science Reviews* **160**, 43–110.
45. Yang Z, Rannala B. 2006 Bayesian estimation of species divergence times under a molecular clock using multiple fossil calibrations with soft bounds. *Molecular Biology and Evolution* **23**, 212–226.
46. Warnock RCM, Yang Z, Donoghue PCJ. 2012 Exploring uncertainty in the calibration of the molecular clock. *Biology Letters* **8**, 156–159.
47. Brown J, Smith S. 2017 The Past Sure Is Tense: On Interpreting Phylogenetic Divergence Time Estimates. *Systematic Biology* **67**, 340–353.
48. Parham JF *et al.* 2012 Best Practices for Justifying Fossil Calibrations. *Systematic Biology* **61**, 346–359.
49. Haug JT, Haug C, Maas A, Kutschera V, Waloszek D. 2010 Evolution of mantis shrimps (Stomatopoda, Malacostraca) in the light of new Mesozoic fossils. *BMC Evolutionary Biology* **10**, 290.
50. Van Der Wal C, Ahyong ST, Ho SYW, Lo N. 2017 The evolutionary history of Stomatopoda (Crustacea: Malacostraca) inferred from molecular data. *PeerJ* **5**, e3844.
51. Maisey JG, Carvalho M da GP de. 1995 First records of fossil sergestid decapods and fossil brachyuran crab larvae (Arthropoda, Crustacea): with remarks on some supposed palaemonid fossils, from the Santana Formation (Aptian-Albian, NE Brazil). *American Museum Novitates* **3132**.
52. Robalino J, Wilkins B, Bracken-Grissom HD, Chan T-Y, O'Leary MA. 2016 The Origin of Large-Bodied Shrimp that Dominate Modern Global Aquaculture. *PLOS ONE* **11**, e0158840.

53. Saraiva AÁF, Pinheiro AP, Santana W. 2018 A remarkable new genus and species of the planktonic shrimp family Luciferidae (Crustacea, Decapoda) from the Cretaceous (Aptian/Albian) of the Araripe Sedimentary Basin, Brazil. *Journal of Paleontology* **92**, 459–465.
54. Van Straelen V. 1933 *Antrimpos madagascariensis*, crustacé décapode du Permotrias de Madagascar. *Bull Mus Roy Hist Nat Belgique* **9**, 1–3.
55. Garassino A, Teruzzi G. 1995 Studies on Permo-Trias of Madagascar, III: The Decapod Crustaceans of the Ambilobe Region (NW Madagascar). *Atti della Società italiana di scienze naturali e del museo civico di storia naturale di Milano* **134**, 85–113.
56. Garassino A, Pasini G. 2002 Studies on Permo-Trias of Madagascar. 5. *Ambilobeia karojoi* n. gen., n. sp. (Crustacea, Decapoda) from the Lower Triassic (Olenekian) of Ambilobe region (NW Madagascar). *Atti della Societaitaliana di Scienze naturali e del Museo Civico di Storia naturale in Milano* **143**, 95–104.
57. Shen Y, Garassino A, Teruzzi G. 2002 Studies on Permo-Trias of Madagascar. 4. Early Triassic conchostracans from Madagascar.
58. Ogg JG. 2012 Triassic. In *The Geologic Time Scale*, pp. 681–730. Elsevier.
59. Garassino A. 2001 New decapod crustaceans from the Cenomanian (Upper Cretaceous) of Lebanon. *Atti Soc. it. Sci. nat. Museo civ. Stor. nat. Milano* **141**, 237–250.
60. Chen C-L, Goy JW, Bracken-Grissom HD, Felder DL, Tsang LM, Chan T-Y. 2016 Phylogeny of Stenopodidea (Crustacea : Decapoda) shrimps inferred from nuclear and mitochondrial genes reveals non-monophyly of the families Spongicolidae and Stenopididae and most of their composite genera. *Invertebrate Systematics* **30**, 479.
61. Jones WT, Feldmann RM, Schweitzer CE, Schram FR, Behr R-A, Hand KL. 2014 The first Paleozoic stenopodidean from the Huntley Mountain Formation (Devonian–Carboniferous), north-central Pennsylvania. *Journal of Paleontology* **88**, 1251–1256.
62. Schram FR, Shen Y, Vonk R, Taylor RS. 2000 The first fossil stenopodidean. *Crustaceana* **73**, 235–242.
63. Wippich MG, Lehmann J. 2004 *Allocrioceras* from the Cenomanian (mid-Cretaceous) of the Lebanon and its bearing on the palaeobiological interpretation of heteromorphic ammonites. *Palaeontology* **47**, 1093–1107.
64. Ogg JG, Hinnov LA, Huang C. 2012 Cretaceous. In *The Geologic Time Scale*, pp. 793–853. Elsevier.
65. Bracken HD, De Grave S, Toon A, Felder DL, Crandall KA. 2010 Phylogenetic position, systematic status, and divergence time of the Procarididea (Crustacea: Decapoda). *Zoologica Scripta* **39**, 198–212.
66. De Grave S, Chan T-Y, Chu KH, Yang C-H, Landeira JM. 2015 Phylogenetics reveals the crustacean order Amphionidacea to be larval shrimps (Decapoda: Caridea). *Scientific Reports* **5**, 17464.
67. Winkler N. 2015 Revision of the fossil crustacean *Blaculla brevipes*, and description of a new caridean shrimp (Crustacea: Decapoda: Dendrobranchiata) from the Upper Jurassic Solnhofen Lithographic Limestones of Schernfeld (Germany). *Zitteliana* , 31–39.
68. Fransen C, De Grave S. 2009 Evolution and radiation of shrimp-like decapods: an overview. In *Decapod Crustacean Phylogenetics* (eds JW Martin, KA Crandall, DL Felder), pp. 246-259. Boca Raton: CRC Press.

69. Christoffersen ML. 1987 Phylogenetic Relationships of Hippolytid Genera, with an Assignment of New Families for the Crangonoidea and Alpheoidea (Crustacea, Decapoda, Caridea). *Cladistics* **3**, 348–362.
70. De Grave S *et al.* 2009 A classification of living and fossil genera of decapod crustaceans. *Raffles Bulletin of Zoology* **21**, 1–109.
71. Bracken HD, De Grave S, Felder DL. 2009 Phylogeny of the infraorder Caridea based on mitochondrial and nuclear genes (Crustacea: Decapoda). In *Decapod Crustacean Phylogenetics* (eds JW Martin, KA Crandall, DL Felder), pp. 281–305. Boca Raton: CRC Press.
72. Aznar-Cormano L, Brisset J, Chan T-Y, Corbari L, Puillandre N, Utge J, Zbinden M, Zuccon D, Samadi S. 2015 An improved taxonomic sampling is a necessary but not sufficient condition for resolving inter-families relationships in Caridean decapods. *Genetica* **143**, 195–205.
73. Schweigert G, Garassino A. 2004 New genera and species of shrimps (Crustacea: Decapoda: Dendrobranchiata, Caridea) from the Upper Jurassic lithographic limestones of S Germany. *Stuttgarter Beiträge zur Naturkunde, Serie B (Geologie und Paläontologie)* **350**, 1–33.
74. Polz H. 2007 Die Garnelengattung *Harthofia* g. nov. (Crustacea: Pleocyemata: Caridea) mit zwei neuen Arten aus den Soln- hofener Plattenkalken von Eichstätt. *Archaeopteryx* **25**, 1–13.
75. Winkler N. 2013 A new genus and species of caridean shrimps from the Upper Jurassic Solnhofen Lithographic Limestones of Schernfeld (S Germany). *Zitteliana* , 77–83.
76. Brayard A *et al.* 2017 Unexpected Early Triassic marine ecosystem and the rise of the Modern evolutionary fauna. *Science Advances* **3**, e1602159.
77. Benton MJ, Donoghue PC, Asher RJ, Friedman M, Near TJ, Vinther J. 2015 Constraints on the timescale of animal evolutionary history. *Palaeontologia Electronica* **18**, 1–106.
78. Tan MH, Gan HM, Dally G, Horner S, Moreno PAR, Rahman S, Austin CM. 2018 More limbs on the tree: mitogenome characterisation and systematic position of ‘living fossil’ species *Neoglyphea inopinata* and *Laurentaeglyphea neocaledonica* (Decapoda : Glypheidea : Glypheidae). *Invertebrate Systematics* **32**, 448-456.
79. Whitfield RP. 1880 Notice of new forms of fossil crustaceans from the Upper Devonian rocks of Ohio, with descriptions of new genera and species. *American Journal of Science* , 33–42.
80. Jones WT, Feldmann RM, Hannibal JT, Schweitzer CE, Garland MC, Maguire EP, Tashman JN. 2018 Morphology and paleoecology of the oldest lobster-like decapod, *Palaeopalaemon newberryi* Whitfield, 1880 (Decapoda: Malacostraca). *Journal of Crustacean Biology.*
81. Feldmann RM, Schweitzer CE, Hu S, Zhang Q, Zhou C, Xie T, Huang J, Wen W. 2012 Macrurous Decapoda from the Luoping Biota (Middle Triassic) of China. *Journal of Paleontology* **86**, 425–441.
82. Bracken-Grissom HD *et al.* 2014 The Emergence of Lobsters: Phylogenetic Relationships, Morphological Evolution and Divergence Time Comparisons of an Ancient Group (Decapoda: Achelata, Astacidea, Glypheidea, Polychelida). *Systematic Biology* **63**, 457–479.

83. Hu S-X, Zhang Q-Y, Chen Z-Q, Zhou C-Y, Lu T, Xie T, Wen W, Huang J-Y, Benton MJ. 2011 The Luoping biota: exceptional preservation, and new evidence on the Triassic recovery from end-Permian mass extinction. *Proceedings of the Royal Society B: Biological Sciences* **278**, 2274–2282.
84. Becker RT, Gradstein FM, Hammer O. 2012 The Devonian Period. In *The Geologic Time Scale*, pp. 559–601. Elsevier.
85. Poore GC. 2016 The names of the higher taxa of Crustacea Decapoda. *Journal of Crustacean Biology* **36**, 248–255.
86. Tshudy D, Sorhannus U. 2000 *Jagtia kunradensis*, a new genus and species of clawed lobster (Decapoda: Nephropidae) from the Upper Cretaceous (Upper Maastrichtian) Maastricht Formation, The Netherlands. *Journal of Paleontology* **74**, 224–229.
87. Karasawa H, Schweitzer CE, Feldmann RM. 2013 Phylogeny and systematics of extant and extinct lobsters. *Journal of Crustacean Biology* **33**, 78–123.
88. Tshudy D, Sorhannus U. 2003 *Hoploparia*, the best-known fossil clawed lobster (Family Nephropidae), is a “wastebasket” genus. *Journal of Crustacean Biology* **23**, 700–711.
89. Feldmann RM, Tshudy DM, Thomson MR. 1993 Late Cretaceous and Paleocene decapod crustaceans from James Ross Basin, Antarctic Peninsula. *Memoir (The Paleontological Society)* 1–41.
90. Molina E *et al.* 2006 The Global Boundary Stratotype Section and Point for the base of the Danian Stage (Paleocene, Paleogene, ‘Tertiary’, Cenozoic) at El Kef, Tunisia — Original definition and revision. *Episodes* **29**, 263.
91. Crandall KA, Harris DJ, Fetzner JW. 2000 The monophyletic origin of freshwater crayfish estimated from nuclear and mitochondrial DNA sequences. *Proceedings of the Royal Society B: Biological Sciences* **267**, 1679–1686.
92. Taylor RS, Schram FR, Shen Y. 1999 A new crayfish family (Decapoda: Astacidea) from the Upper Jurassic of China, with a reinterpretation of other Chinese crayfish taxa. *Paleontological Research* **3**, 121–136.
93. Tsang LM, Lin F-J, Chu KH, Chan T-Y. 2008 Phylogeny of Thalassinidea (Crustacea, Decapoda) inferred from three rDNA sequences: implications for morphological evolution and superfamily classification. *Journal of Zoological Systematics and Evolutionary Research* **46**, 216–223.
94. Robles R, Tudge CC, Dworschak PC, Poore GCB, Felder DL. 2009 Molecular phylogeny of the Thalassinidea based on nuclear and mitochondrial genes. In *Decapod Crustacean Phylogenetics* (eds JW Martin, KA Crandall, DL Felder), p. 309. Boca Raton: CRC Press.
95. Woodward H. 1876 On some new macrurous Crustacea from the Kimmeridge Clay of the Sub-Wealden Boring, Sussex, and from Boulogne-sur-Mer. *Quarterly Journal of the geological Society* **32**, 47–50.
96. Breton G, Carpentier C, Huault V, Lathuilière B. 2003 Decapod crustaceans from the Kimmeridgian of Bure (Meuse, France). *Contributions to Zoology* **72**, 91–94.
97. Hyžnỳ M, Klompmaker AA. 2015 Systematics, phylogeny, and taphonomy of ghost shrimps (Decapoda): a perspective from the fossil record. *Arthropod Systematics & Phylogeny* **73**, 401.
98. Ogg JG, Hinnov LA, Huang C. 2012 Jurassic. In *The Geologic Time Scale*, pp. 731–791. Elsevier.

99. Karasawa H. 1993 Cenozoic decapod Crustacea from southwest Japan. *Bulletin of the Mizunami Fossil Museum* **20**, 1–92.
100. Paiva TS, Tavares M, Silva-Neto ID. 2010 Removing the homonymy between *Laurentiella* Dragesco & Njine, 1971 (Protista) and *Laurentiella* Le Loeuff & Intès, 1974 (Crustacea). *Crustaceana* **83**, 767–768.
101. Tomida Y, Nakaya H, Saegusa H, Miyata K, Fukuchi A. 2013 Miocene land mammals and stratigraphy of Japan. In *Mammalian Biostratigraphy and Chronology of Asia*.
102. Karasawa H. 1999 The Cenozoic decapod crustacean fauna of southwest Japan. In *Proceedings of the Fourth International Crustacean Congress*, pp. 29–41.
103. Bracken-Grissom HD, Cannon ME, Cabezas P, Feldmann RM, Schweitzer CE, Ahyong ST, Felder DL, Lemaitre R, Crandall KA. 2013 A comprehensive and integrative reconstruction of evolutionary history for Anomura (Crustacea: Decapoda). *BMC Evolutionary Biology* **13**, 128.
104. Robins CM, Feldmann RM, Schweitzer CE. 2012 The oldest Munididae (Decapoda: Anomura: Galatheoidea) from Ernstbrunn, Austria (Tithonian). *Annalen des Naturhistorischen Museums in Wien. Serie A für Mineralogie und Petrographie, Geologie und Paläontologie, Anthropologie und Prähistorie* , 289–300.
105. Robins CM, Feldmann RM, Schweitzer CE. 2013 Nine new genera and 24 new species of the Munidopsidae (Decapoda: Anomura: Galatheoidea) from the Jurassic Ernstbrunn Limestone of Austria, and notes on fossil munidopsid classification. *Annalen des Naturhistorischen Museums in Wien. Serie A für Mineralogie und Petrographie, Geologie und Paläontologie, Anthropologie und Prähistorie* , 167–251.
106. Schweitzer CE, Feldmann RM. 2010 Earliest known Porcellanidae (Decapoda: Anomura: Galatheoidea) (Jurassic: Tithonian). *Neues Jahrbuch für Geologie und Paläontologie - Abhandlungen* **258**, 243–248.
107. Schneider S, Harzhauser M, Kroh A, Lukeneder A, Zuschin M. 2013 Ernstbrunn Limestone and Klentnice beds (Kimmeridgian-Berriasian; Waschberg-Ždánice Unit; NE Austria and SE Czech Republic): state of the art and bibliography. *Bulletin of Geosciences* , 105–130.
108. Moshammer B, Schlagintweit F. 1999 The Erstbrunn Limestone (Lower Austria): New data on biostratigraphy and applied geology. In *Geologie ohne Grenzen: Festschrift 150 Jahre Geologische Bundesanstalt* (eds H Lobitzer, P Grecula), Wien: Geologische Bundesanstalt.
109. Chablais J, Feldmann RM, Schweitzer CE. 2011 A new Triassic decapod, *Platykotta akaina*, from the Arabian shelf of the northern United Arab Emirates: earliest occurrence of the Anomura. *Paläontologische Zeitschrift* **85**, 93–102.
110. Hegna TA, Luque J, Wolfe JM. In press. The fossil record of the Pancrustacea. In *Evolution and Biogeography* (eds GCB Poore, M Thiel), Oxford: Oxford University Press.
111. Fraaije RHB, Klompmaker AA, Artal P. 2012 New species, genera and a family of hermit crabs (Crustacea, Anomura, Paguroidea) from a mid-Cretaceous reef of Navarra, northern Spain. *Neues Jahrbuch für Geologie und Paläontologie - Abhandlungen* **263**, 85–92.
112. Karasawa H, Mizuno Y, Hachiya K, Ando Y. 2017 Reappraisal of anomuran and brachyuran decapods from the lower Miocene Morozaki Group, Japan, collected by the Tokai Fossil Society. *Bulletin of the Mizunami Fossil Museum* **43**.
113. Noever C, Glenner H. 2017 The origin of king crabs: hermit crab ancestry under the magnifying glass. *Zoological Journal of the Linnean Society.*

114. Tsang LM, Chan T-Y, Ahyong ST, Chu KH. 2011 Hermit to King, or Hermit to All: Multiple Transitions to Crab-like Forms from Hermit Crab Ancestors. *Systematic Biology* **60**, 616–629.
115. Feldmann RM. 1998 *Paralomis debodeorum* , a new species of decapod crustacean from the Miocene of New Zealand: First notice of the Lithodidae in the fossil record. *New Zealand Journal of Geology and Geophysics* **41**, 35–38.
116. Barron JA, Browning J, Sugarman P, Miller KG. 2013 Refinement of late-Early and Middle Miocene diatom biostratigraphy for the East Coast of the United States. *Geosphere* **9**, 1286–1302.
117. Tsang LM, Schubart CD, Ahyong ST, Lai JCY, Au EYC, Chan T-Y, Ng PKL, Chu KH. 2014 Evolutionary History of True Crabs (Crustacea: Decapoda: Brachyura) and the Origin of Freshwater Crabs. *Molecular Biology and Evolution* **31**, 1173–1187.
118. Luque J. 2015 The oldest higher true crabs (Crustacea: Decapoda: Brachyura): insights from the Early Cretaceous of the Americas. *Palaeontology* **58**, 251–263.
119. Feldmann RM, Schweitzer CE. 2010 Is *Eocarcinus* Withers, 1932, a Basal Brachyuran? *Journal of Crustacean Biology* **30**, 241–250.
120. Haug C, Haug JT. 2014 *Eoprosopon klugi* (Brachyura)–the oldest unequivocal and most “primitive” crab reconsidered. *Palaeodiversity.*
121. Schubart CD, Cannicci S, Vannini M, Fratini S. 2006 Molecular phylogeny of grapsoid crabs (Decapoda, Brachyura) and allies based on two mitochondrial genes and a proposal for refraining from current superfamily classification. *Journal of Zoological Systematics and Evolutionary Research* **44**, 193–199.
122. Müller P, Collins JSH. 1991 Late Eocene coral-associated decapods (Crustacea) from Hungary. *Mededelingen van de Werkgroep voor Tertiaire en Kwartaire Geologie* **28**, 47–92.
123. Schweitzer CE, Karasawa H. 2004 Revision of *Amydrocarcinus* and *Palaeograpsus* (Decapoda: Brachyura: Xanthoidea) with definition of three new genera. *Paleontological Research* **8**, 71–86.
124. Luque J, Schweitzer CE, Santana W, Portell RW, Vega FJ, Klompmaker AA. 2017 Checklist of fossil decapod crustaceans from tropical America. Part I: Anomura and Brachyura. *Nauplius* **25**.
125. Vega FJ, Cosma T, Coutiño MA, Feldmann RM, Nyborg TG, Schweitzer CE, Waugh DA. 2001 New Middle Eocene Decapods (Crustacea) from Chiapas, México. *Journal of Paleontology* **75**, 929–946.
126. Vega FJ, Nyborg T, Coutiño MA, Hernández-Monzón O. 2008 Review and additions to the Eocene decapod Crustacea from Chiapas, Mexico. *Bulletin of the Mizunami Fossil Museum* **34**, 51–71.
127. Tsang LM, Ahyong ST, Shih H-T, Ng PKL. 2018 Further polyphyly of pinnotheroid crabs: the molecular phylogenetic position of the polychaete-associated Aphanodactylidae. *Invertebrate Systematics* **32**, 92.
128. Palacios-Theil E, Cuesta JA, Campos E, Felder DL. 2009 Molecular genetic re-examination of subfamilies and polyphyly in the family Pinnotheridae (Crustacea: Decapoda). In *Decapod Crustacean Phylogenetics* (eds JW Martin, KA Crandall, DL Felder), Boca Raton: CRC Press.

129. Palacios Theil E, Cuesta JA, Felder DL. 2016 Molecular evidence for non-monophyly of the pinnotheroid crabs (Crustacea: Brachyura: Pinnotheroidea), warranting taxonomic reappraisal. *Invertebrate Systematics* **30**, 1.
130. Karasawa H, Kato H. 2001 The systematic status of the genus *Miosesarma* Karasawa, 1989 with a phylogenetic analysis within the family Grapsidae and a review of fossil records (Crustacea: Decapoda: Brachyura). *Paleontological Research* **5**, 259–275.
131. Donovan SK. 2010 A field guide to the Cretaceous and Cenozoic fossil decapod crustacean localities of Jamaica. *Caribbean Journal of Science* **46**, 39–53.
132. Ozsvárt P, Kocsis L, Nyerges A, Győri O, Pálfy J. 2016 The Eocene-Oligocene climate transition in the Central Paratethys. *Palaeogeography, Palaeoclimatology, Palaeoecology* **459**, 471–487.
133. Evans N. 2018 Molecular phylogenetics of swimming crabs (Portunoidea Rafinesque, 1815) supports a revised family-level classification and suggests a single derived origin of symbiotic taxa. *PeerJ* **6**, e4260.
134. Klompmaker AA. 2013 Extreme diversity of decapod crustaceans from the mid-Cretaceous (late Albian) of Spain: Implications for Cretaceous decapod paleoecology. *Cretaceous Research* **41**, 150–185.
135. Hultgren KM, Stachowicz JJ. 2008 Molecular phylogeny of the brachyuran crab superfamily Majoidea indicates close congruence with trees based on larval morphology. *Molecular Phylogenetics and Evolution* **48**, 986–996.
136. Hultgren KM, Guerao G, Marques FPL, Palero FP. 2009 Assessing the contribution of molecular and larval morphological characters in a combined phylogenetic analysis of the superfamily Majoidea. In *Decapod Crustacean Phylogenetics* (eds JW Martin, KA Crandall, DL Felder), pp. 437–455. Boca Raton: CRC Press.
137. Windsor AM, Felder DL. 2014 Molecular phylogenetics and taxonomic reanalysis of the family Mithracidae MacLeay (Decapoda : Brachyura : Majoidea). *Invertebrate Systematics* **28**, 145.
138. Artal P, Van Bakel BWM, Onetti A. 2014 A new inachid crab (Brachyura, Majoidea) from the Middle Eocene of the provinces of Barcelona and Girona (Catalonia, Spain) *Planobranchia palmuelleri* n. sp. *Scripta Geologica.*
139. Feldmann RM, Schweitzer CE, Baltzly LM, Bennett OA, Jones AR, Mathias FF, Weaver KL, Yost SL. 2013 New and previously known decapod crustaceans from the Late Cretaceous of New Jersey and Delaware, USA. *Bulletin of the Mizunami Fossil Museum* **39**, 7–37.
140. Feldmann RM, Maxwell PA. 1990 Late Eocene decapod Crustacea from North Westland, South Island, New Zealand. *Journal of Paleontology* **64**, 779–797.
141. Aguilera O, Rodrigues de Aguilera D, Vega FJ, Sánchez-Villagra M. 2010 Mesozoic and Cenozoic decapod crustaceans from Venezuela and related trace-fossil assemblages. *Urumaco and Venezuelan Paleontology* , 103–128.
142. Schweitzer CE, Feldmann RM, Gonzáles-Barba G, Vega FJ. 2002 New crabs from the Eocene and Oligocene of Baja California Sur, Mexico and an assessment of the evolutionary and paleobiogeographic implications of Mexican fossil decapods. *Journal of Paleontology* **76**, 1–43.
143. Serra Kiel J *et al.* 2003 An inventory of the marine and transitional Middle/Upper Eocene deposits of the Southeastern Pyrenean Foreland Basin (NE Spain). *Geologica Acta* **1**.

144. Lai JCY, Mendoza JCE, Guinot D, Clark PF, Ng PKL. 2011 Xanthidae MacLeay, 1838 (Decapoda: Brachyura: Xanthoidea) systematics: A multi-gene approach with support from adult and zoeal morphology. *Zoologischer Anzeiger* **250**, 407–448.
145. Milne Edwards A. 1862 Monographie des Crustacés fossiles de la famille des Cancériens. *Annales des Sciences Naturelles, Zoologie* **4**, 31–85.
146. Busulini A, Tessier G, Beschin C. 2006 The genus *Phlyctenodes* Milne Edwards, 1862 (Crustacea: Decapoda: Xanthidae) in the Eocene of Europe. *Revista mexicana de ciencias geológicas* **23**, 350–360.
147. Karasawa H, Schweitzer CE. 2006 A new classification of the Xanthoidea sensu lato (Crustacea Decapoda: Brachyura) based on phylogenetic analysis and traditional systematics and evaluation of all fossil Xanthoidea *sensu lato*. *Contributions to Zoology* **75**.
148. Thoma BP, Guinot D, Felder DL. 2014 Evolutionary relationships among American mud crabs (Crustacea: Decapoda: Brachyura: Xanthoidea) inferred from nuclear and mitochondrial markers, with comments on adult morphology. *Zoological Journal of the Linnean Society* **170**, 86–109.
149. de Angeli A, Garassino A. 2002 Galatheid, chirostylid and porcellanid decapods (Crustacea, Decapoda, Anomura) from the Eocene and Oligocene of Vicenza (N Italy). *Mem. Soc. it. Sci. nat. Mus. civ. Storia nat. Milano* **30**, 1–40.
150. De Angeli A, Garassino A. 2014 *Palinurellus bericus* n. sp. (Crustacea, Decapoda, Palinuridae) from the late Eocene (Priabonian) of San Feliciano (Orgiano, Vicenza, northeastern Italy). *Natural History Sciences* **1**, 7.

Figure S1. Workflow for our AHE data collection and analysis. Yellow boxes represent published genomic resources, blue boxes are newly sequenced in this paper, and red boxes are the focal results in **Figures 2-3**.

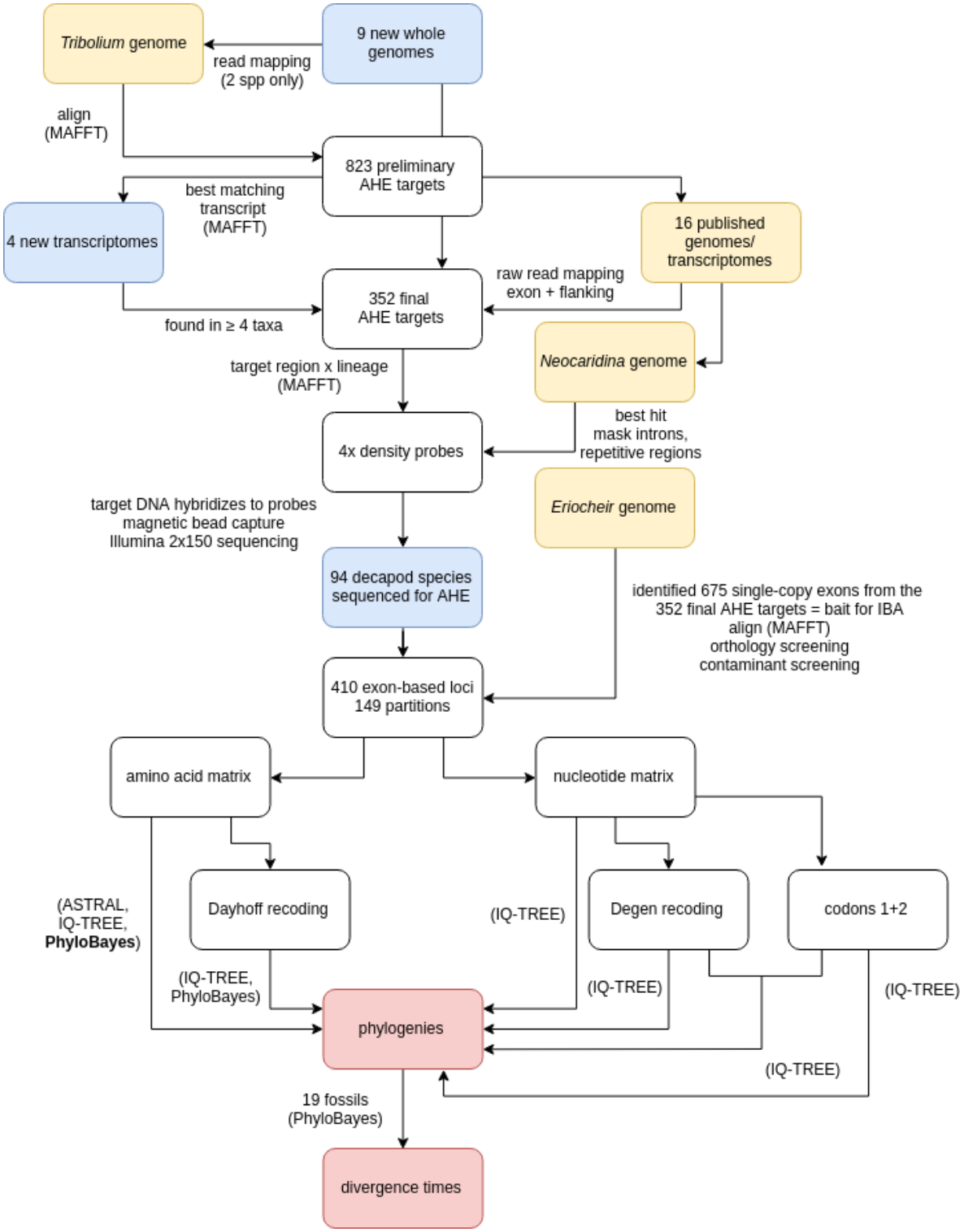

Figure S2. Pairwise heat map of species-pairwise amino acid dataset completeness for all 410 exon-based loci, in the unrecoded amino acid dataset. Numbers in parentheses are total exon-based loci captured per species. Low shared site coverage in shades of red and high shared site coverage in shades of green.

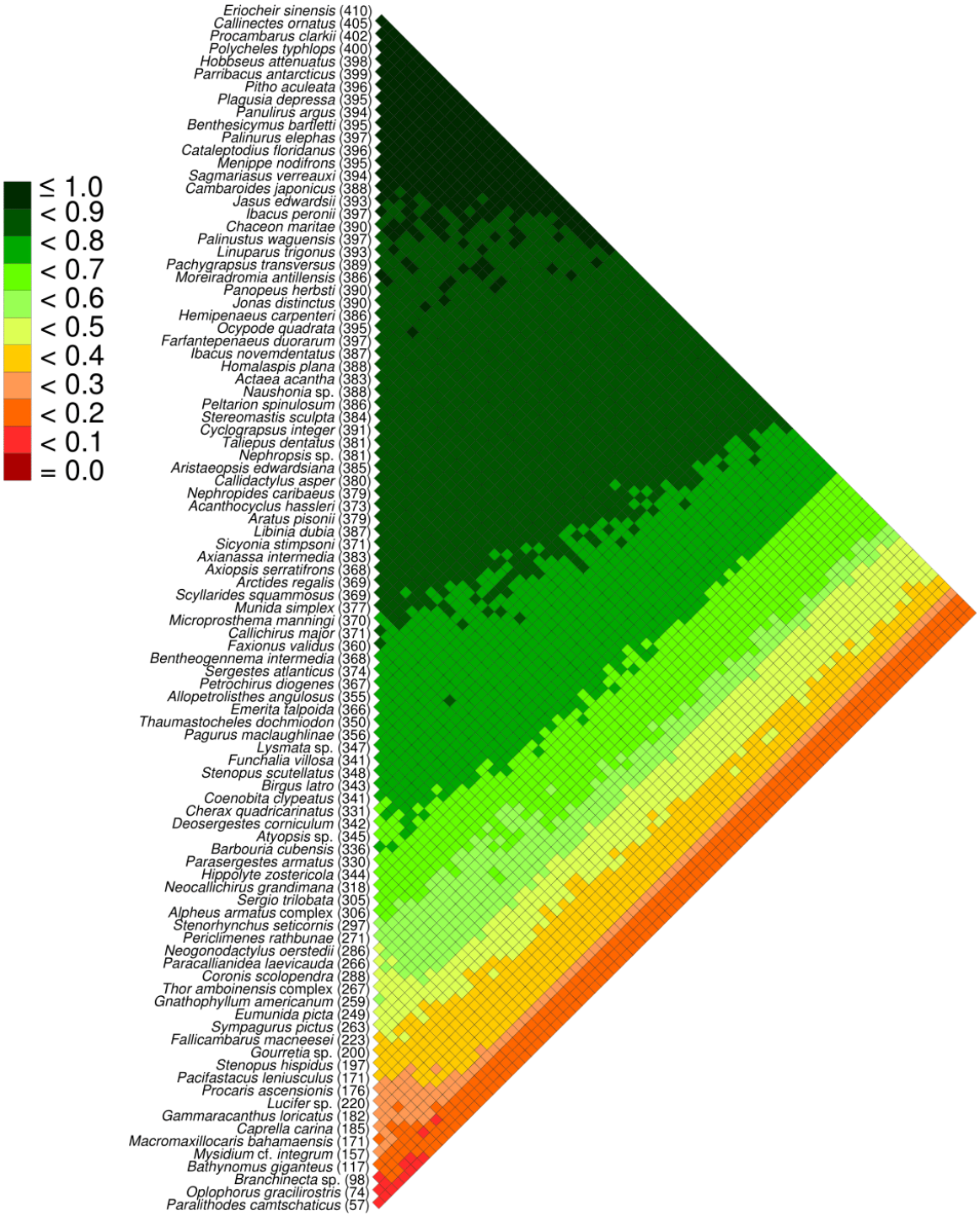

Figure S3. Phylogenetic hypothesis for Decapoda based on the topology from the ML partitioned amino acid analysis. Values at nodes represent nonparametric bootstraps. Unlabeled nodes are considered strongly supported.

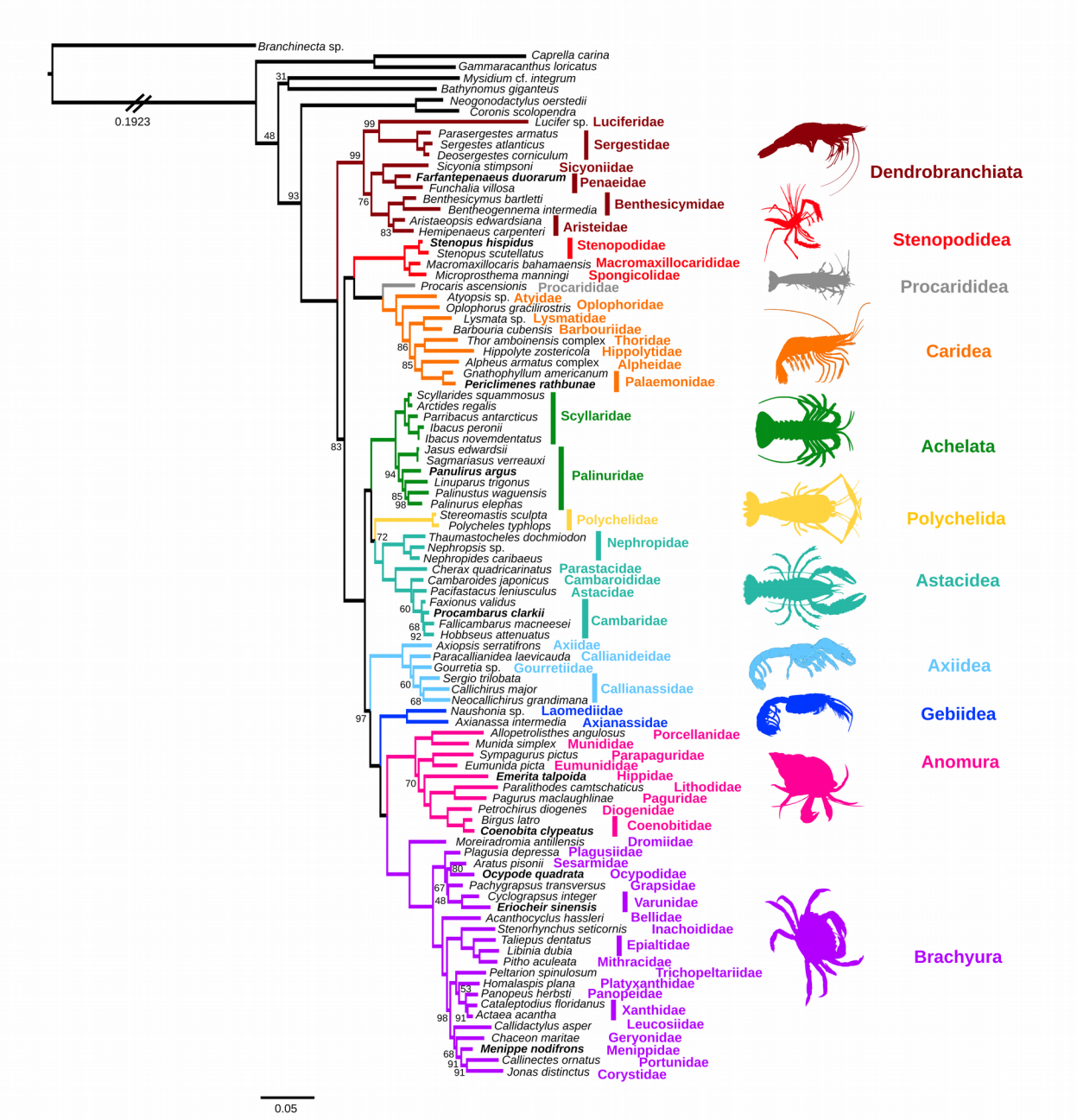

Figure S4. Phylogenetic hypothesis for Decapoda based on the topology from the Bayesian CAT-GTR+G analysis with Dayhoff-6 recoding. Values at nodes represent posterior probabilities. Unlabeled nodes are considered strongly supported.

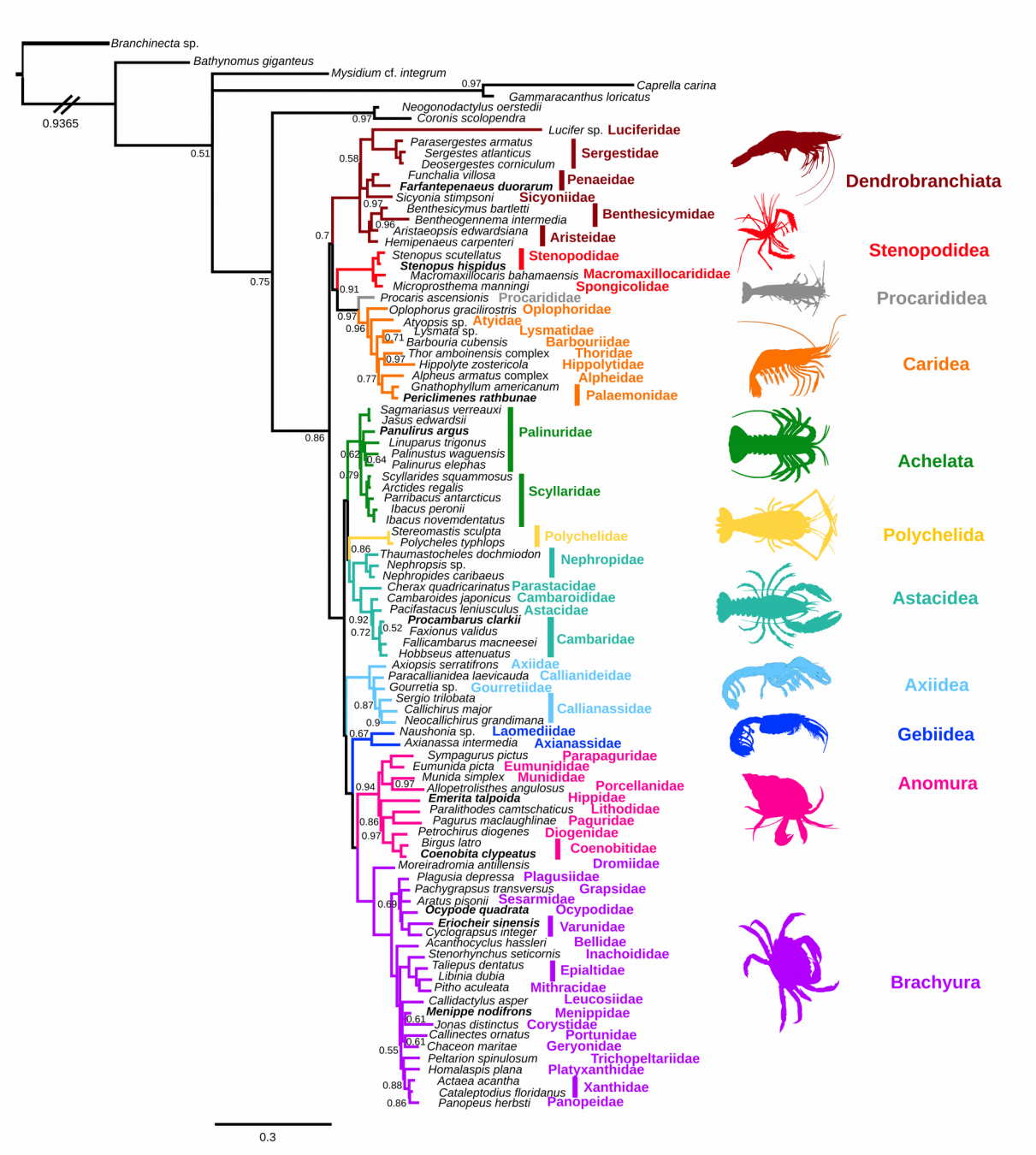

Figure S5. Phylogenetic hypothesis for Decapoda based on the topology from the ML partitioned amino acid analysis with Dayhoff-6 recoding. Values at nodes represent nonparametric bootstraps. Unlabeled nodes are considered strongly supported.

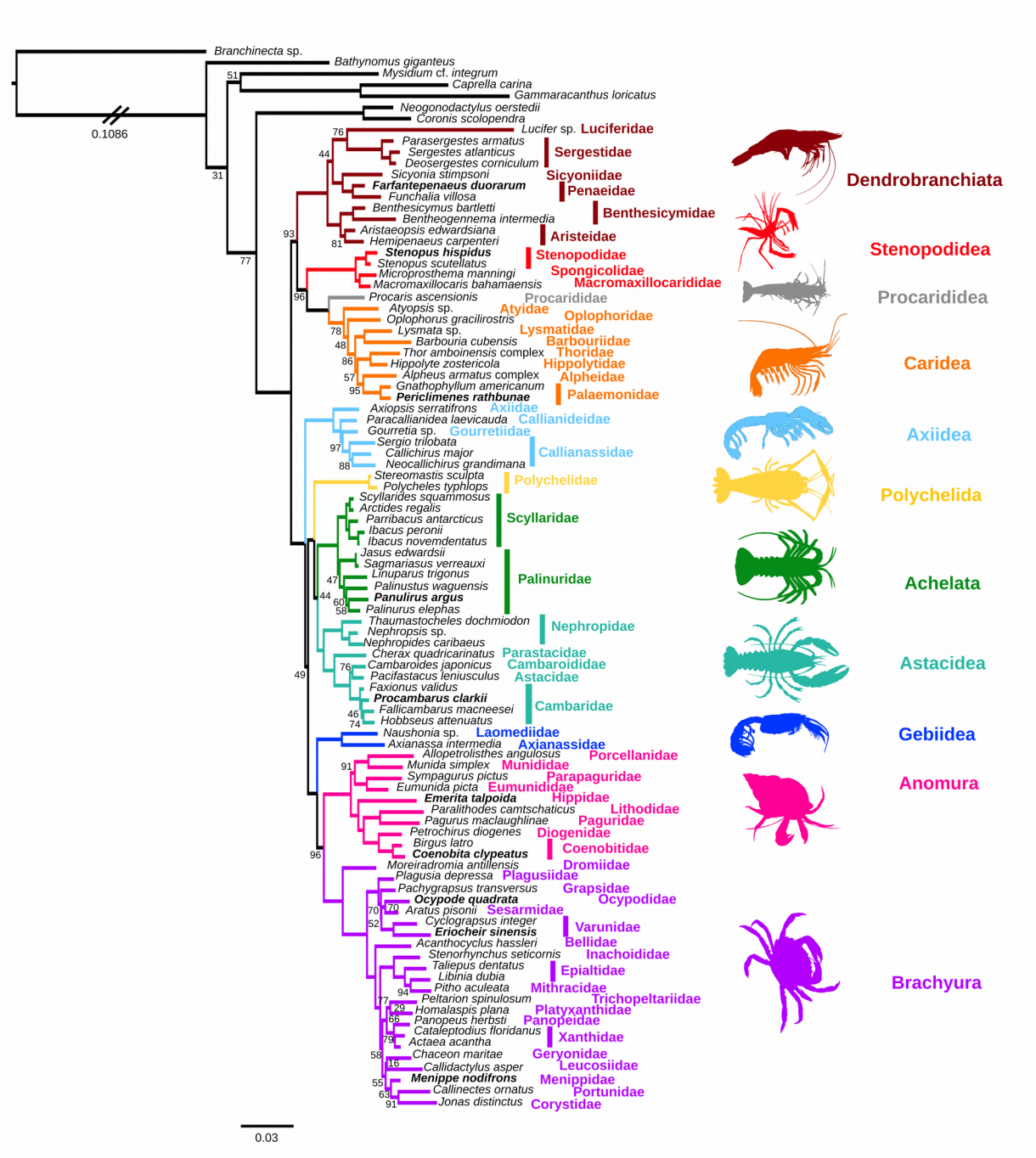

Figure S6. Phylogenetic hypothesis for Decapoda based on the topology from ASTRAL species tree analysis. Values at nodes represent quartet node support. Unlabeled nodes are considered strongly supported, following posterior probabilities (i.e. ≥ 0.98 for strong support).

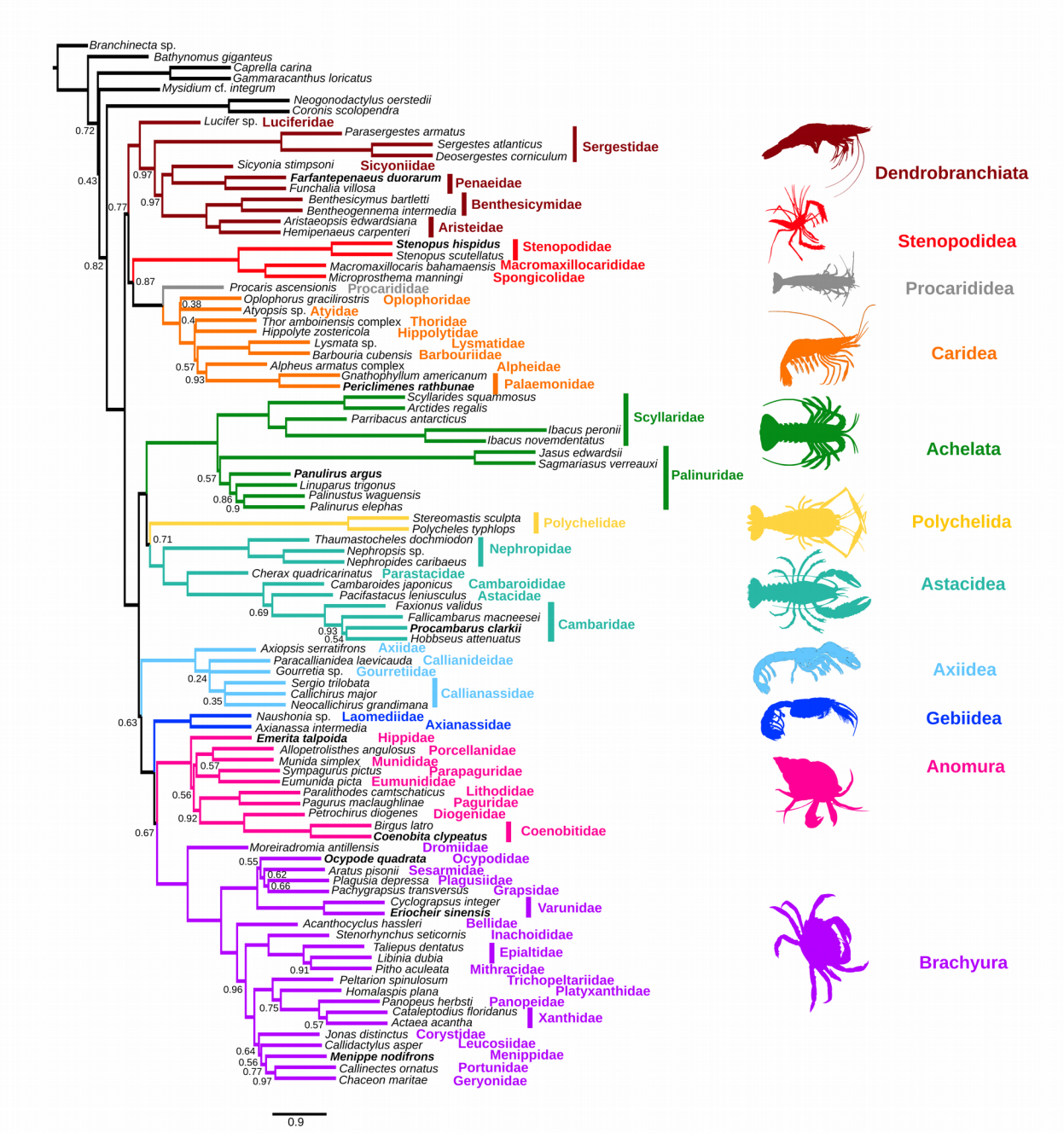

Figure S7. Phylogenetic hypothesis for Decapoda based on the topology from the ML partitioned nucleotide analysis. Values at nodes represent nonparametric bootstraps. Unlabeled nodes are considered strongly supported.

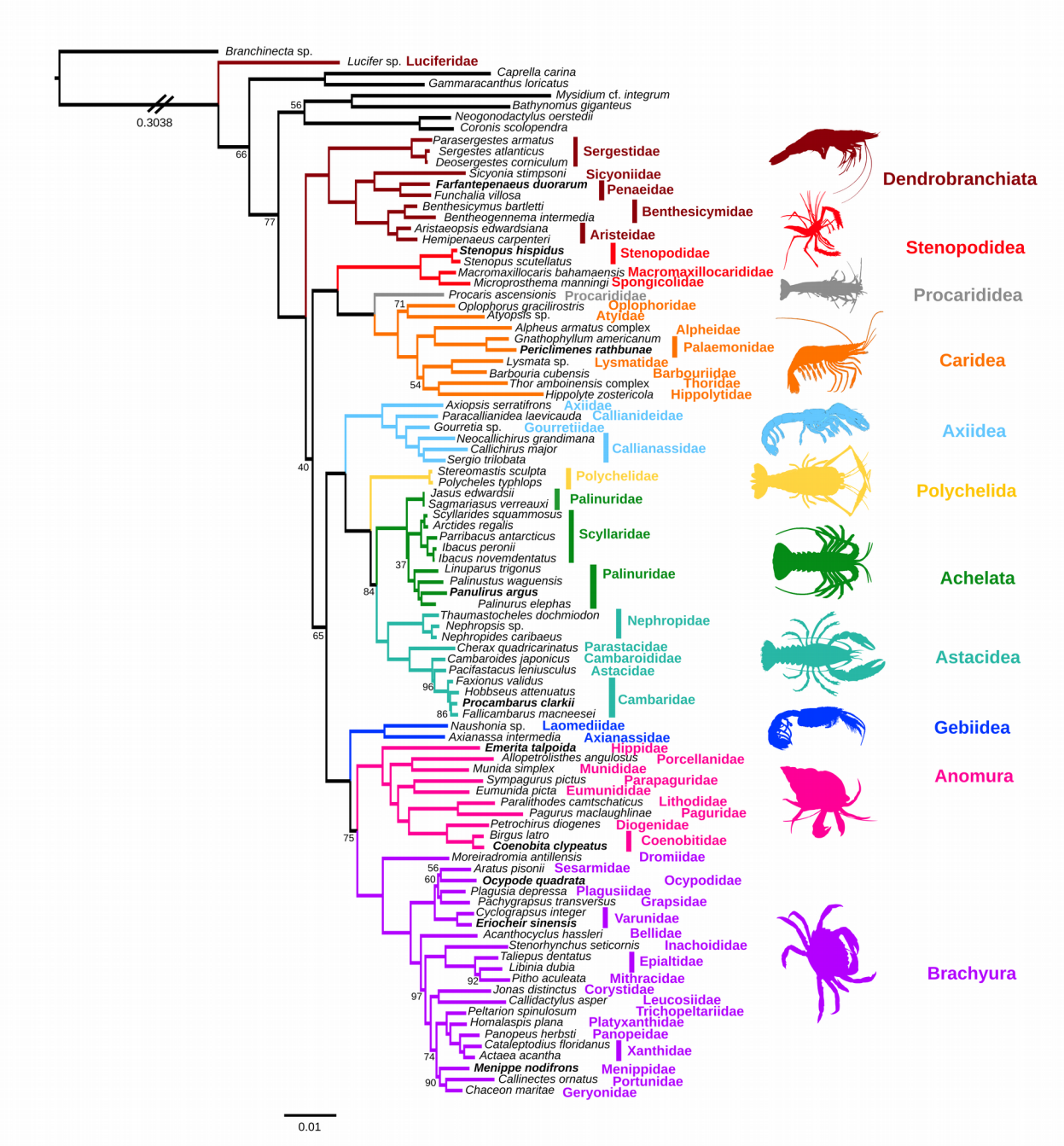

Figure S8. Phylogenetic hypothesis for Decapoda based on the topology from the ML partitioned nucleotide analysis with only codon positions 1+2 included. Values at nodes represent nonparametric bootstraps. Unlabeled nodes are considered strongly supported.

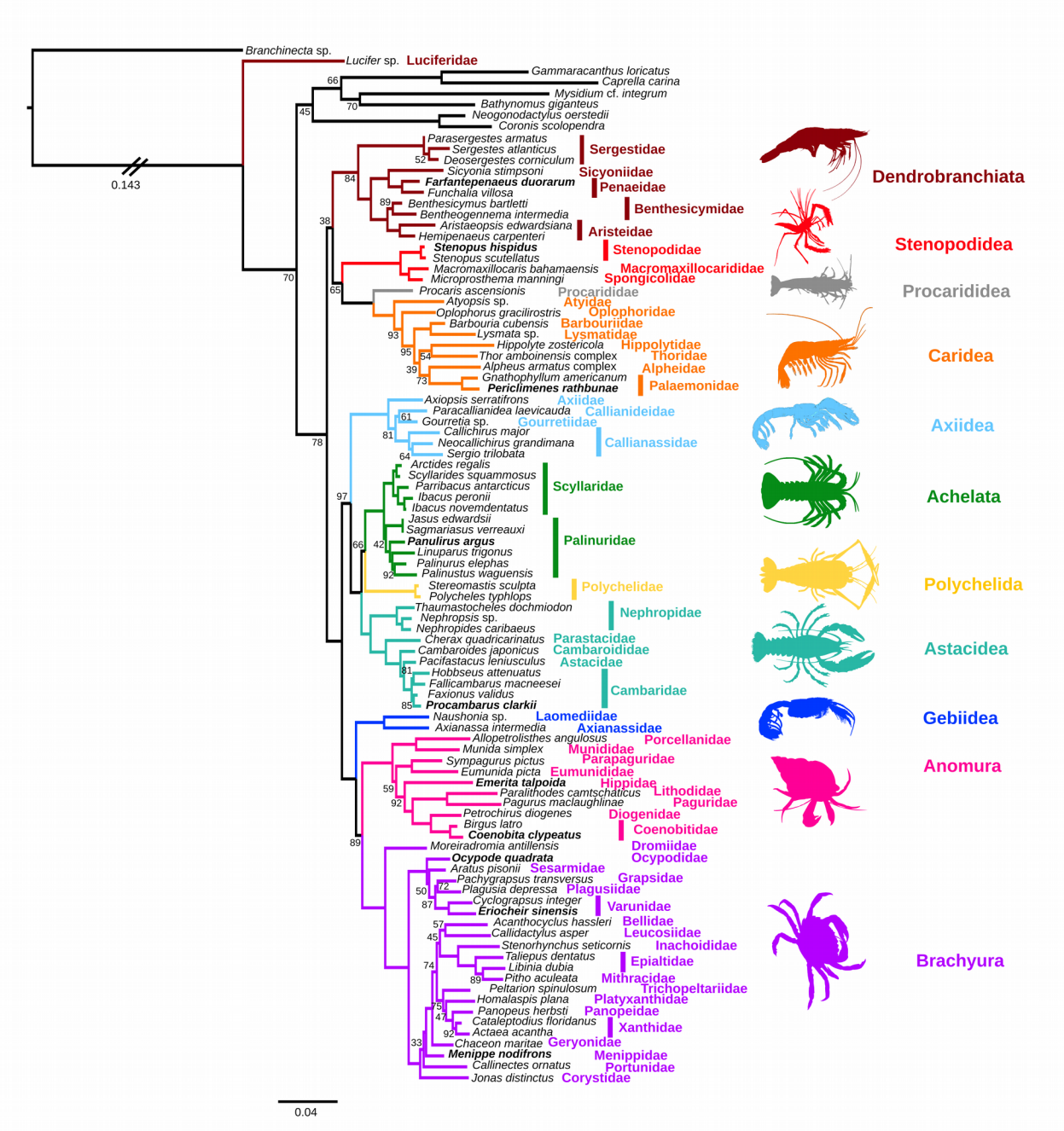

Figure S9. Phylogenetic hypothesis for Decapoda based on the topology from the ML partitioned nucleotide analysis with Degen recoding. Values at nodes represent nonparametric bootstraps. Unlabeled nodes are considered strongly supported.

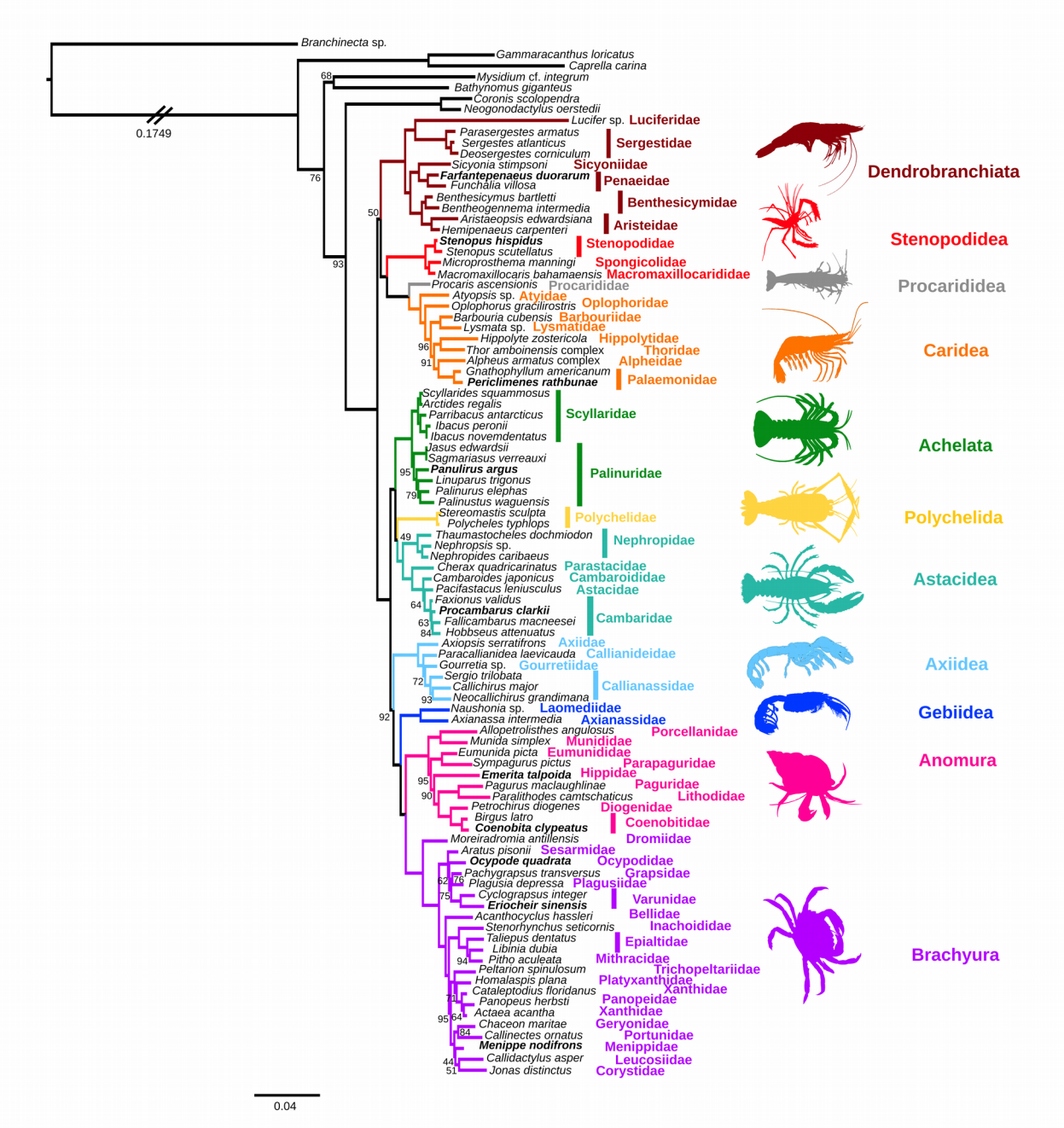

Figure S10. Phylogenetic hypothesis for Decapoda based on the topology from the ML partitioned nucleotide analysis with Degen recoding and only codon positions 1+2 included. Values at nodes represent nonparametric bootstraps. Unlabeled nodes are considered strongly supported.

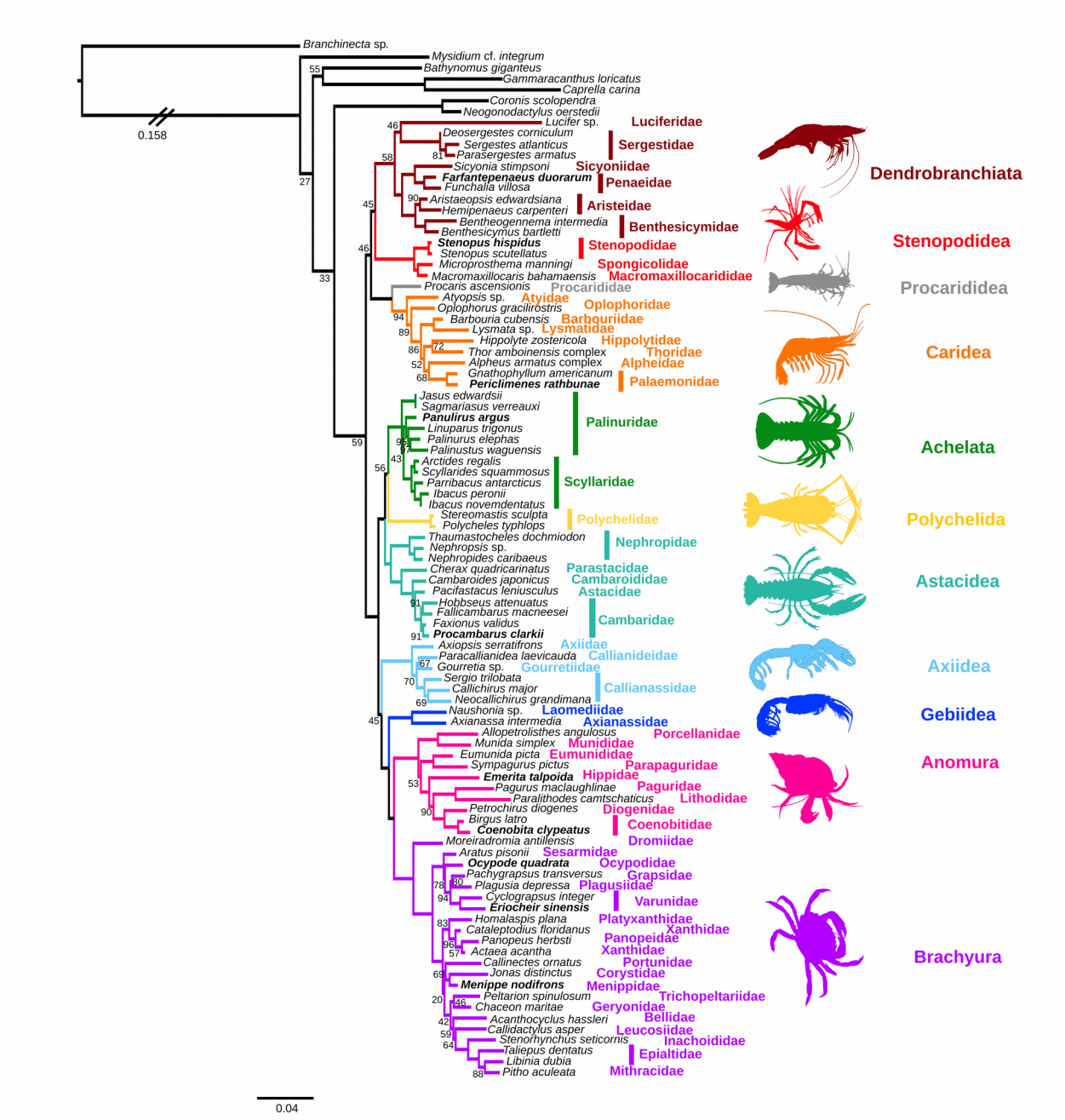

Figure S11. Saturation plot for each codon position with transversions (v) and transitions (s) plotted against F84 distance. The third codon position clearly deviates from expected values, and thus has experienced saturation.

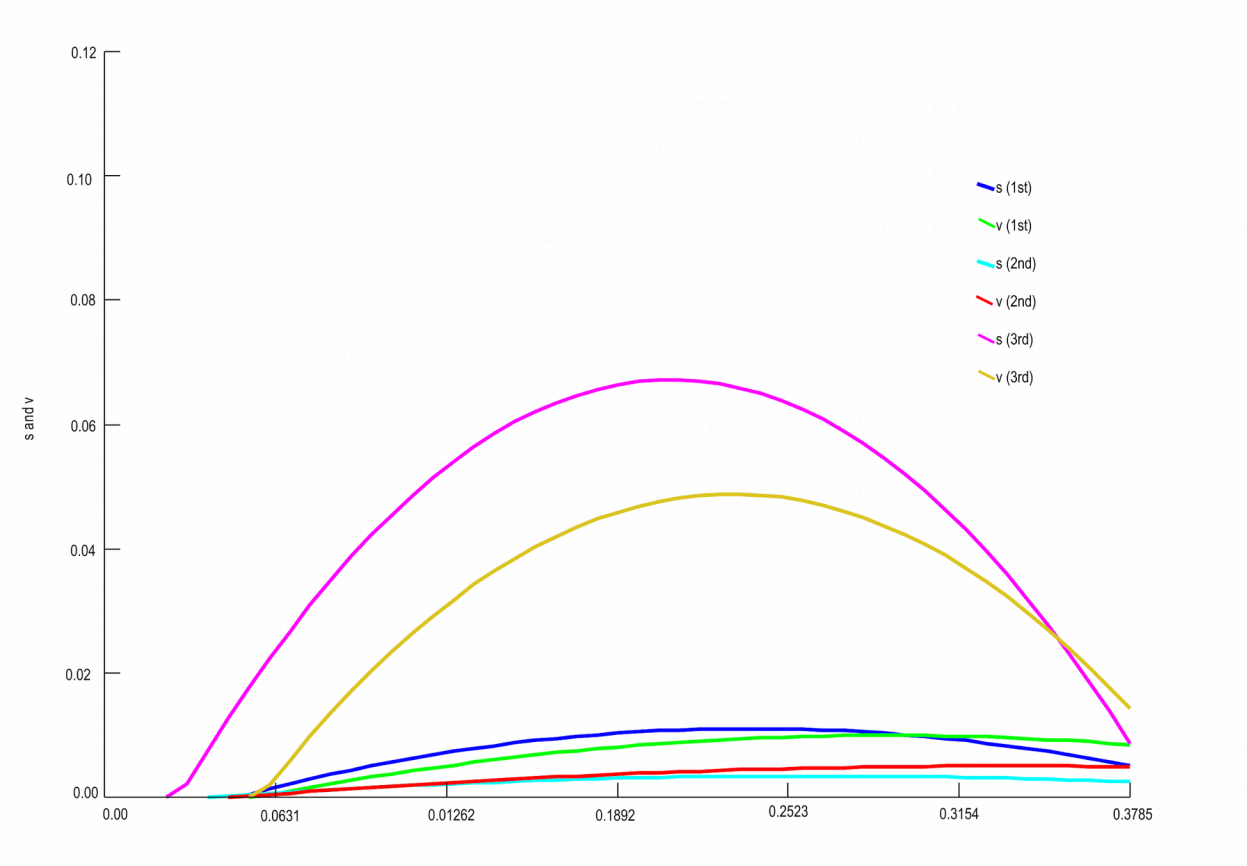

Figure S12. Divergence time estimates for Decapoda based on the topology in **Figure 2**. Posterior ages were estimated in PhyloBayes using the CAT-GTR+G substitution model, the UGAM clock model, and a gamma distributed root prior of 440 Ma ± 20 Myr. Horizontal shaded bars represent 95% confidence intervals. Numbered circles represent nodes with fossil calibrations.

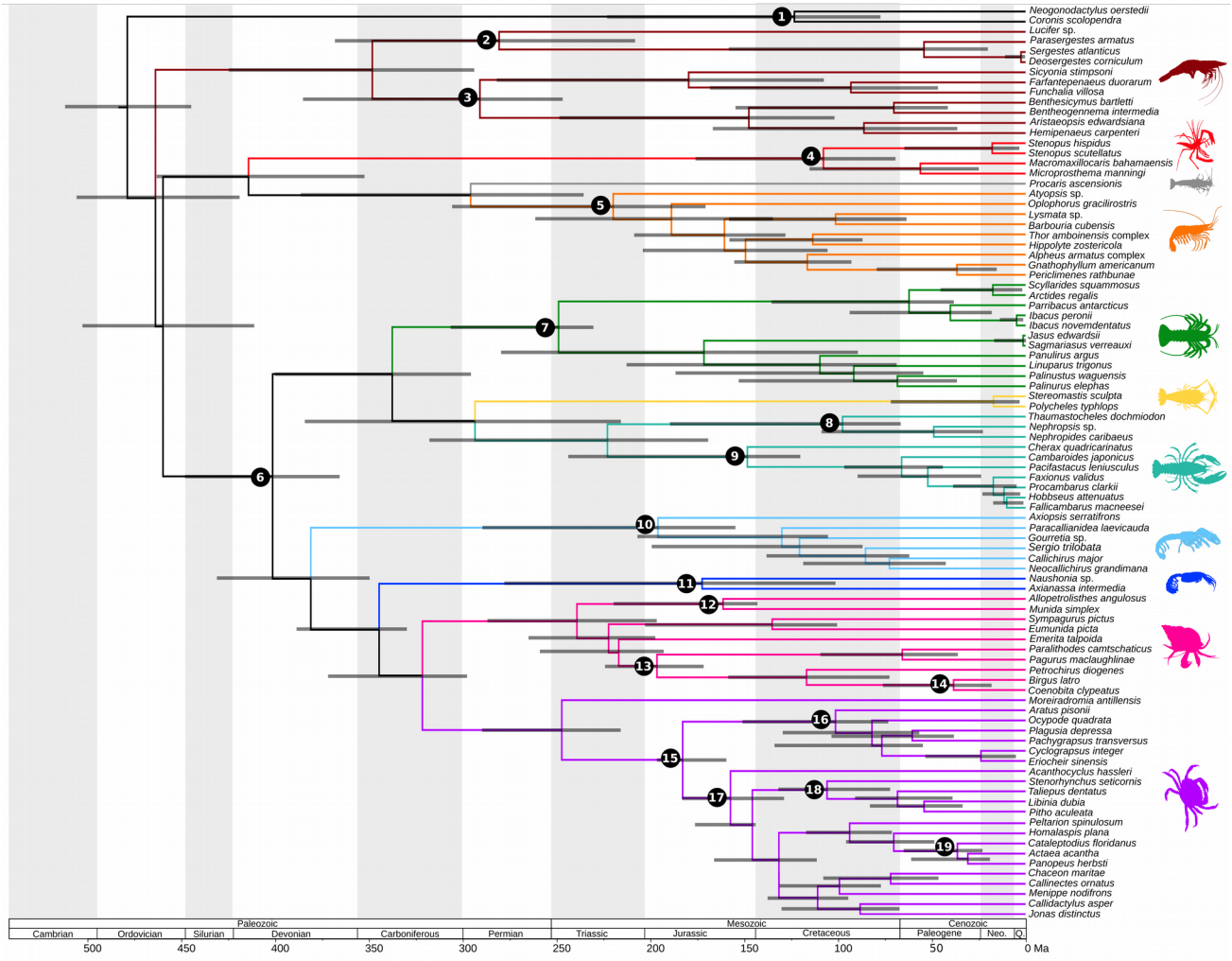

Figure S13. Comparison of posterior probability distributions for divergence times assessed as in Figure 3 (posterior), and using the same analyses under the effective prior (removing sequence data). The posterior analyses are shaded; effective priors are superimposed on the same axes with a heavy line of the same color. Grey/black analyses with the CIR autocorrelated clock model (depicted in Figure 3); orange analyses with the UGAM uncorrelated clock model. *(a)* Selected nodes directly calibrated by fossils and their calibration number; *(b)* Selected nodes calibrated by only a birth-death tree prior.

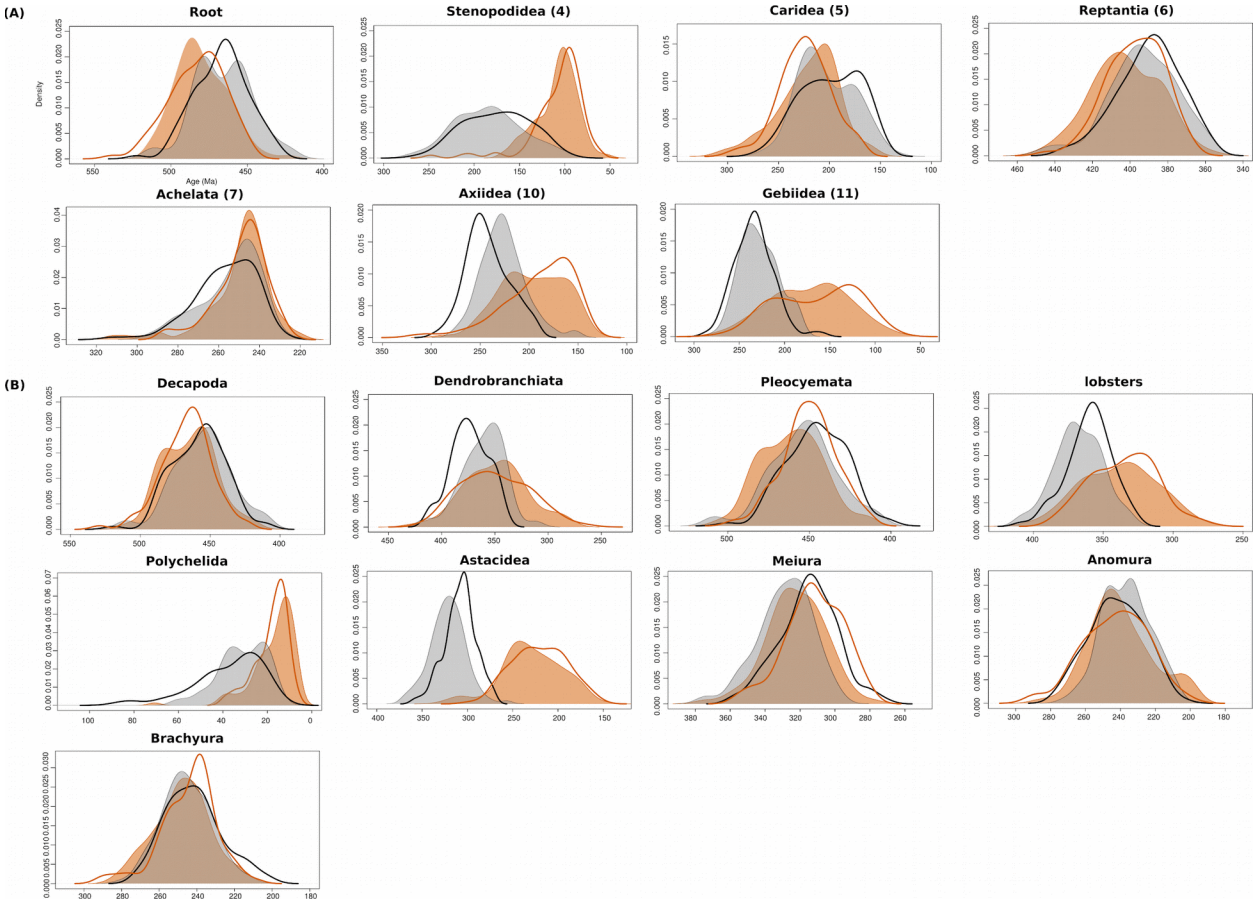

All Extended Tables are available as .xslx or .csv files attached.

Table S1. Details of all transcriptome and genome sequences used in probe design.

Table S2. Sample information for whole genome sequencing, including SRA accession information.

Table S3. Sample information for transcriptome sequencing, including SRA accession information.

Table S4. Assembly statistics for transcriptome sequencing.

Table S5. Brief description of enrichment kits for each of six selected major lineages (Achelata, Anomura, Astacidea, Brachyura, Caridea, and Dendrobranchiata).

Table S6. Sample information for AHE sequencing, including SRA accession information.

Table S7. Formatted list of node calibration priors.

Table S8. Assembly statistics for AHE sequencing, and exon-based loci sequenced for each species. For each locus, 1 represents presence and 0 represents absence in the main data matrix.